measured proviral load over the course of the treatment and found that it decreased dramatically within 2 weeks (Figure 7B). Thus, this demonstrates that mogamulizumab can indeed reduce the number of STLV-1-infected cells *in vivo*.

Eight weeks after the final administration of mogamulizumab, the proviral load started to recover (Figure 7B). To investigate whether mogamulizumab influences the clonality of STLV-1-infected cells, we evaluated the absolute number of each clone by high-throughput sequencing of provirus integration sites. Figure 7C shows changes of the five most abundant clones at weeks 0, 5 and 18. The major clones before the treatment (week 0) recovered at week 18 (red lines in Figure 7C), while some clones were present constantly during the treatment (grey lines) or diminished after the treatment (blue lines). Interestingly, some clones (green lines) that emerged in a monkey after treatment were rare or even not detected before treatment (Figure 7C).

## Discussion

HTLV-1 is thought to originate from STLV-1. In STLV-1-infected monkeys, investigators found clonal proliferation of STLV-1-infected cells and the preferential infection of $CD4^+$ T cells by the virus [15,31]. Moreover, several groups reported the development of lymphomas in STLV-1-infected monkeys [16,17,32-35]. Monoclonal integration of STLV-1 in the lymphoproliferative disease of African green monkeys was detected by Southern blot [16,33], demonstrating the direct causative role of STLV-1. Thus STLV-1-infected non-human primates have been thought to be a useful animal model for HTLV-1 research. The dynamics of infected cells after treatment with histone deacetylase inhibitors and reverse transcriptase inhibitors has been analyzed in STLV-1-infected baboons, and it was found that this combination significantly decreased proviral load in treated animals [36]. However, there have been no detailed studies on functions of STLV-1-encoded genes. Analyses of the functions of its accessory and regulatory proteins are necessary if we are to use STLV-1-infected monkeys as a model of HTLV-1 infection. In the present study, we focused on Japanese macaques naturally infected with STLV-1.

The amino acid sequence of STLV-1 Tax is closely homologous to that of HTLV-1 Tax, and this study demonstrated that their functions on various transcriptional pathways are similar as well. This study was the first to identify SBZ as an antisense transcript of STLV-1 and a homolog of HBZ. SBZ and HBZ share only approximately 73% identity at the amino acid level. Nevertheless, for all the functions we examined, SBZ behaves similarly to HBZ. In particular, SBZ expression could induce Foxp3 expression like HBZ expression does. This might be attributed to the following reasons. First, the N-terminal region, as well as the heptad repeats of hydrophobic amino acids in the basic leucine zipper domain, are conserved between HBZ and SBZ. This may allow SBZ to interact with and suppress NF-κB, AP-1 and other transcription factors with basic leucine zipper motifs [37,38]. Second, the LXXLL-like region (Leu27, Leu28, Leu48 and Leu49), which is critical for the interaction with p300 and Smad3 protein, is also conserved between HBZ and SBZ [22,39]. Some lysine residues present in HBZ are substituted with different amino acids in Japanese macaque SBZ. This study showed that SBZ has similar functions compared with HBZ, suggesting that these lysine residues are not critical for their functions. However, further studies are necessary for deep understanding of implication of these amino acid sequences.

HTLV-1 increases the number of infected cells by clonal proliferation of infected cells, which likely facilitates cell-to-cell transmission of this virus. Clonal proliferation of STLV-1-infected cells in Celebes macaques was demonstrated by the conventional inverse PCR method [15]. However, this technique could detect only a limited population of the clones because of its limited sensitivity or the stochastic amplification of the integration sites. In the present study, we investigated more comprehensively the clonal proliferation of infected cells in Japanese macaques naturally infected with STLV-1 by massively sequencing the unique integration sites of the provirus. The finding that STLV-1-infected cells proliferated clonally in the monkeys with higher proviral loads resembles the finding for HTLV-1. Furthermore, one monkey had lymphoma in the brain, showing that STLV-1 induces lymphoma in Japanese macaques. Analyses of STLV-1 integration sites in this T-cell lymphoma showed that one of the major clones in the brain was unique to this tumor, suggesting that this clone played an important role in the lymphomagenesis of this tumor.

This study also revealed a remarkable difference in STLV-1 seroprevalence between Japanese macaques (320/533: 60%) and rhesus macaques (1/163: 0.6%). Previous studies showed that the seroprevalence in rhesus macaques was 25%, and that in Japanese macaques was quite high [40-42]. Similarly, high seroprevalence was reported in baboons [43]. Furthermore, many studies reported the development of lymphoma in baboons [17,44,45]. The high seroprevalence and the development of lymphomas in Japanese macaques and baboons may suggest a higher susceptibility of these species to STLV-1 infection. Japanese macaques and baboons infected with STLV-1 may be suitable models for HTLV-1 research.

In this study, we also demonstrated that mogamulizumab strongly suppressed proviral load in STLV-1-infected Japanese macaques. Proviral load was suppressed for 4 weeks after the final administration of mogamulizumab, which seems reasonable when considering that the half-life of the

antibody administered at 1.0 mg/kg is approximately 18 days as measured in a clinical trial [46]. Some STLV-1-infected major clones recovered after the treatment, while other clones were still suppressed or even not detected. In HTLV-1-infected individuals, HTLV-1 proviral load is relatively constant in the chronic phase, although some minor clones fluctuate [25]. This study is the first to report that most of the major clones recover after the withdrawal of mogamulizumab. This observation suggests that the major clones may have some growth advantages that allow them to proliferate robustly *in vivo*. These growth advantages may be due to the integration site of the provirus, accumulation of genetic mutations, or epigenetic changes. The population of some clones remained constant over the course of the treatment. We speculate that these clones are negative for CCR4 expression. High proviral load is associated with risk of ATL and inflammatory diseases. Therefore, suppression of proviral load by mogamulizumab is a possible treatment for HTLV-1-associated inflammatory diseases such as HAM/TSP.

## Conclusions

In summary, this study is the first to show that STLV-1 Tax and SBZ have activities similar to those of Tax and HBZ, activities which likely induce clonal proliferation and T-cell lymphoma in infected monkeys. STLV-1-infected Japanese macaques appear to be a good model for studying the effects of anti-viral drugs and the immunological aspects of HTLV-1 infection.

## Methods

### Biological samples of macaques

Japanese macaques (*Macaca fuscata*) and rhesus macaques (*Macaca mulatta*) used in this study were reared in the Primate Research Institute, Kyoto University. Blood samples were obtained from the macaques (for routine veterinary and microbiological examination) under ketamine anesthesia. All animal studies were conducted in accordance with the protocols of experimental procedures that were approved (2011–095) by the Animal Welfare and Animal Care Committee of the Primate Research Institute of Kyoto University, Inuyama, Japan.

### Antibody screening and measurement of proviral load

Plasma samples were screened for the presence of antibodies against HTLV-1 by particle-agglutination test using SERODIA-HTLV-1 (Fujirebio). Proviral load was measured by real-time PCR quantifying the copy number of *tax* and *RAG1* as previously described [47]. Primers and probes are available in Additional file 4.

### Detection of STLV-1 transcripts

Total RNA was extracted from STLV-1-infected Japanese macaque cell line Si-2 [48] with Trizol (Invitrogen), then cDNA was synthesized with SuperScript III (Invitrogen) using oligo dT primer. STLV-1 *tax* and *SBZ* was detected by PCR using primers (see Additional file 4) from the synthesized Si-2 cDNA: for STLV-1 *tax*, 2 min at 95°C, followed by 35 cycles of 20 seconds at 95°C, 10 seconds at 61°C, and 30 seconds at 72°C, and additional 5 min at 72°C; for SBZ, 2 min at 95°C, followed by 35 cycles of 20 seconds at 95°C, 10 seconds at 58°C, and 30 seconds at 72°C, and additional 5 min at 72°C. For comparison, HTLV-1 *tax* and *HBZ* were also amplified by PCR using cDNA of HTLV-1-infected cell lines (MT-1 or MT-2) with the same conditions. The primers used are shown in Additional file 4.

### Plasmids

The PathDetect pNFκB-Luc, pAP-1-Luc and pNFAT-Luc plasmids were purchased from Stratagene. The 3TP-Lux, TopFlash reporter plasmids and WT-Luc were described previously [22,49]. The coding sequences of STLV-1 Tax and SBZ were amplified from STLV-1 provirus using oligos (see Additional file 4) and cloned into pME18Sneo to generate expression plasmids of STLV-1 Tax and SBZ. HTLV-1 tax was amplified using flanking primers (see Additional file 4) from pCGTax [50] and subcloned into pME18Sneo. The expression vector of HBZ cloned into pME18Sneo was described previously [11]. For the reporter assay, Jurkat cells or HepG2 cells were co-transfected with the reporter plasmid and the viral protein expression plasmids specified in each experiment, as previously described [22,24,51]. The activity of firefly luciferase was represented by normalizing to that of Renilla luciferase.

### Retroviral vectors

The SBZ coding fragment was inserted into pGCDNSamI/N utilizing the NotI and SalI sites and SBZ-expressing retroviral vector was prepared as described previously [22].

### Transduction of primary T-cells with retroviral vectors

$CD4^+CD25^-$ mouse T lymphocytes were stimulated and transduced with SBZ-expressing retroviral vector as previously described [22]. Forty-eight hours after the transduction, cells were harvested and analyzed by flow cytometry.

### Flow cytometry

Antibodies used in this study were as follows: anti-human CD4 (OKT4), anti-Tax MI-73 [52], anti-mouse CD4 (RM4-5), anti-human CD271 (NGFR) (C40-1457), anti-mouse Foxp3 (FJK-16s), anti-human CD3 (SP34-2) and anti-human CCR4 (1G1, which recognizes a different epitope from that recognized by mogamulizumab). Intracellular staining was performed as previously described for Tax [52] and Foxp3 [22]. Cells were analyzed

by BD FACSCanto II with FACS Diva Software (BD Biosciences) or BD FACSVerse with FACSuite software (BD Biosciences).

### Deep sequencing of provirus integration sites

The provirus integration sites in the Japanese macaque genome were amplified by linker-mediated PCR as previously described [27], with some modifications. Japanese macaque PBMC genomic DNA (3 μg) was sheared by sonication with a Bioruptor UCD-200 TM to obtain DNA fragments of approximately 200–500 bp. The ends of the DNA fragments were repaired to generate blunt ends using 18 units of T4 DNA polymerase, 5.3 units of DNA Klenow Polymerase I and 18 units of T4 polynucleotide kinase (TOYOBO) in T4 DNA ligase buffer (NEB) supplemented with 300 μM each of dNTP (TAKARA Bio). Adenine nucleotides were added to the blunt ends, and then linkers were ligated using 24 units of T4 DNA ligase (TOYOBO) in T4 DNA ligase buffer (NEB) utilizing the overhang of one thymidine nucleotide at the 3' end of the linker. The linker was generated by annealing two oligonucleotides (see Additional file 4). The first round of PCR was performed with the primers, STLV-1 Bio5 and Bio4. STLV-1 Bio5 anneals to the sequence within LTR of the STLV-1 provirus and Bio4 is the sequence present in the linker (see Additional file 4). Then, nested PCR was performed with the primers, Ion A-Bio7 and P1. In Ion A-Bio7, uppercase letters denote the sequence that anneals to the viral LTR downstream of STLV-1 Bio5, whereas the sequence in lowercase letters represents a tag specific for the Ion Torrent Personal Genome Machine (Ion PGM). P1 is also a tag specific for Ion PGM, which appears in the linker sequence (see Additional file 4). The amplification conditions of both the first and second PCR were 96°C for 30 sec, 7 cycles of 94°C for 5 sec and 72°C for 1 min, 23 cycles of 94°C for 5 sec and 68°C for 1 min, followed by additional 68°C for 9 min. Amplified fragments of approximately 150–300 bp were size-selected with E-Gel SizeSelect Agarose Gel (Life Technologies) and used as a DNA library in subsequent deep sequencing. Template beads to be sequenced with Ion Torrent Personal Genome Machine (Ion PGM) were prepared with the DNA library using the Ion PGM 200 Xpress Template Kit (Applied Biosystems) and subjected to sequencing on Ion Torrent 314 or 316 semiconductor chip using Ion PGM 200 Sequencing Kit (Applied Biosystems).

### Deep sequencing data analysis

The host genomic sequences, located between the region immediately adjacent to the viral 3' LTR (ACACA) and the linker sequence (AGATCG), were extracted from the reads. Reads that started with GTTGGG (viral 5' LTR) were removed. Remaining reads were mapped to the reference genome of *Macaca mulatta* (MMUL 1.0) using the Burrows-Wheeler Aligner (BWA) [53]. Reads that were mapped only to single sites were analyzed. In order to obtain the absolute frequency of each provirus clone (the number of sister cells of the clone), the end position of each mapped read was obtained from the start position and cigar code in the SAM file generated by BWA. The reads with an identical start position and end position (integration site and shear site) were judged to derive from a single DNA fragment amplified by PCR, while reads with identical integration sites but distinct shear sites were judged to derive from different cells in a clone. In other words, the number of reads in the second category reflects the absolute frequency of each clone. Relative frequency represents the proportion of the absolute frequency of a clone to the number of all the sister cells observed. In order to minimize the distortion of relative frequencies of major clones, 6,000 reads that were mapped only to single sites were randomly selected for each specimen and analyzed (see Additional file 2).

### Treatment of STLV-1$^+$ Japanese macaques with humanized anti-CCR4 antibody

Two Japanese macaques infected with STLV-1 were treated with mogamulizumab, which is an antibody against CCR4 and is approved in Japan as a drug to treat relapsed ATL. Mogamulizumab was provided by Kyowa Hakko Kirin Co Ltd. One mg/kg mogamulizumab was diluted in 40 ml saline and infused into each monkey intravenously for 20 min. Administration was performed once a week for 4 times. Before each administration, a 10 ml of blood sample was obtained. After the fourth administration, blood samples were collected every 2 weeks until week 11. Extra samples were collected on week 15 and week 18. The two monkeys were observed for any adverse effects during the experiment.

## Additional files

**Additional file 1: Phylogenetic analyses of HTLV-1 subtypes and Japanese macaque STLV-1.**

**Additional file 2: Deep sequencing data analysis.**

**Additional file 3: In vitro staining of Japanese macaque PBMCs with mogamulizumab.**

**Additional file 4: Primers and oligonucleotides.**

#### Competing interests

Kyowa Hakko Kirin provided us the monoclonal antibody (mogamulizumab) that was used in this study.

#### Authors' contributions

JY and M. Matsuoka conceived of this study. JT carried out antibody screening and proviral load measurement. M. Miura, KS, GM and TZ carried out the molecular experiments and the reporter assays. AK, AW, AS and HA coordinated the macaque experiments and collected the macaque specimens. PM analyzed viral protein and surface marker expression. KO carried out immunohistochemistry and pathological analyses. M. Miura carried out massive sequencing and its data analysis. M. Miura, JY and M.

Matsuoka prepared the manuscript. All the authors approved the final manuscript.

**Acknowledgements**
We thank Masakazu Shimizu for technical support on massive sequencing with Ion Torrent PGM, Mayumi Morimoto and Yoshiro Kamanaka for technical assistance on monkey experiments, Linda Kingsbury for proof-reading, and Charles Bangham, and Heather Niederer for valuable advice on analyses of integration sites. This study was supported by a Grant-in-aid for Scientific Research from the Ministry of Education, Science, Sports, and Culture of Japan (221S0001), a grant from SENSHIN medical research foundation, a grant from Japan Leukaemia Research Fund to MM, and the Cooperation Research Program of the Primate Research Institute, Kyoto University.

**Author details**
[1]Laboratory of Virus Control, Institute for Virus Research, Kyoto University, Shogoin Kawahara-cho 53, Sakyo-ku, Kyoto 606-8507, Japan. [2]Department of Pathology, School of Medicine, Kurume University, Kurume, Fukuoka, Japan. [3]Center for Human Evolution Modeling Research, Primate Research Institute, Kyoto University, Inuyama, Aichi, Japan. [4]Present address: College of Chemistry and Life Sciences, Zhejiang Normal University, Jinhua, China.

Received: 18 August 2013 Accepted: 15 October 2013
Published: 24 October 2013

**References**

1. Gallo RC: **The discovery of the first human retrovirus: HTLV-1 and HTLV-2.** *Retrovirology* 2005, **2**:17.
2. Takatsuki K: **Discovery of adult T-cell leukemia.** *Retrovirology* 2005, **2**:16.
3. Gessain A, Cassar O: **Epidemiological aspects and world distribution of HTLV-1 infection.** *Front Microbiol* 2012, **3**:388.
4. Matsuoka M, Jeang KT: **Human T-cell leukaemia virus type 1 (HTLV-1) infectivity and cellular transformation.** *Nat Rev Cancer* 2007, **7**:270–280.
5. Gessain A, Boeri E, Yanagihara R, Gallo RC, Franchini G: **Complete nucleotide sequence of a highly divergent human T-cell leukemia (lymphotropic) virus type I (HTLV-I) variant from melanesia: genetic and phylogenetic relationship to HTLV-I strains from other geographical regions.** *Front Microbiol* 1993, **67**:1015–1023.
6. Osame M, Usuku K, Izumo S, *et al*: **HTLV-I associated myelopathy, a new clinical entity.** *Lancet* 1986, **1**:1031–1032.
7. Mochizuki M, Yamaguchi K, Takatsuki K, Watanabe T, Mori S, Tajima K: **HTLV-I and uveitis.** *Lancet* 1992, **339**:1110.
8. Bangham CR: **CTL quality and the control of human retroviral infections.** *Eur J Immunol* 2009, **39**:1700–1712.
9. Kawano N, Shimoda K, Ishikawa F, *et al*: **Adult T-cell leukemia development from a human T-cell leukemia virus type I carrier after a living-donor liver transplantation.** *Transplantation* 2006, **82**:840–843.
10. Tamaki H, Matsuoka M: **Donor-derived T-cell leukemia after bone marrow transplantation.** *N Engl J Med* 2006, **354**:1758–1759.
11. Satou Y, Yasunaga J, Yoshida M, Matsuoka M: **HTLV-I basic leucine zipper factor gene mRNA supports proliferation of adult T cell leukemia cells.** *Proc Natl Acad Sci U S A* 2006, **103**:720–725.
12. Hanon E, Hall S, Taylor GP, *et al*: **Abundant tax protein expression in CD4+ T cells infected with human T-cell lymphotropic virus type I (HTLV-I) is prevented by cytotoxic T lymphocytes.** *Blood* 2000, **95**:1386–1392.
13. Macnamara A, Rowan A, Hilburn S, *et al*: **HLA class I binding of HBZ determines outcome in HTLV-1 infection.** *PLoS Pathog* 2010, **6**:e1001117.
14. Watanabe T, Seiki M, Tsujimoto H, Miyoshi I, Hayami M, Yoshida M: **Sequence homology of the simian retrovirus genome with human T-cell leukemia virus type I.** *Virology* 1985, **144**:59–65.
15. Gabet AS, Gessain A, Wattel E: **High simian T-cell leukemia virus type 1 proviral loads combined with genetic stability as a result of cell-associated provirus replication in naturally infected, asymptomatic monkeys.** *Int J Cancer* 2003, **107**:74–83.
16. Tsujimoto H, Noda Y, Ishikawa K, *et al*: **Development of adult T-cell leukemia-like disease in African green monkey associated with clonal integration of simian T-cell leukemia virus type I.** *Cancer Res* 1987, **47**:269–274.
17. Voevodin A, Samilchuk E, Schatzl H, Boeri E, Franchini G: **Interspecies transmission of macaque simian T-cell leukemia/lymphoma virus type 1 in baboons resulted in an outbreak of malignant lymphoma.** *J Virol* 1996, **70**:1633–1639.
18. Cavanagh MH, Landry S, Audet B, *et al*: **HTLV-I antisense transcripts initiating in the 3'LTR are alternatively spliced and polyadenylated.** *Retrovirology* 2006, **3**:15.
19. Sun SC, Yamaoka S: **Activation of NF-kappaB by HTLV-I and implications for cell transformation.** *Oncogene* 2005, **24**:5952–5964.
20. Hall WW, Fujii M: **Deregulation of cell-signaling pathways in HTLV-1 infection.** *Oncogene* 2005, **24**:5965–5975.
21. Matsuoka M: **HTLV-1 bZIP factor gene: its roles in HTLV-1 pathogenesis.** *Mol Aspects Med* 2010, **31**:359–366.
22. Zhao T, Satou Y, Sugata K, *et al*: **HTLV-1 bZIP factor enhances TGF-{beta} signaling through p300 coactivator.** *Blood* 2011, **118**:1865–1876.
23. Satou Y, Yasunaga J, Zhao T, *et al*: **HTLV-1 bZIP factor induces T-cell lymphoma and systemic inflammation in vivo.** *PLoS Pathog* 2011, **7**:e1001274.
24. Ma G, Yasunaga J, Fan J, Yanagawa S, Matsuoka M: **HTLV-1 bZIP factor dysregulates the Wnt pathways to support proliferation and migration of adult T-cell leukemia cells.** *Oncogene* 2013, **32**:4222–4230.
25. Etoh K, Tamiya S, Yamaguchi K, *et al*: **Persistent clonal proliferation of human T-lymphotropic virus type I-infected cells in vivo.** *Cancer res* 1997, **57**:4862–4867.
26. Wattel E, Vartanian JP, Pannetier C, Wain-Hobson S: **Clonal expansion of human T-cell leukemia virus type I-infected cells in asymptomatic and symptomatic carriers without malignancy.** *J Virol* 1995, **69**:2863–2868.
27. Gillet NA, Malani N, Melamed A, *et al*: **The host genomic environment of the provirus determines the abundance of HTLV-1-infected T-cell clones.** *Blood* 2011, **117**:3113–3122.
28. Yoshie O, Fujisawa R, Nakayama T, *et al*: **Frequent expression of CCR4 in adult T-cell leukemia and human T-cell leukemia virus type 1-transformed T cells.** *Blood* 2002, **99**:1505–1511.
29. Ishii T, Ishida T, Utsunomiya A, *et al*: **Defucosylated humanized anti-CCR4 monoclonal antibody KW-0761 as a novel immunotherapeutic agent for adult T-cell leukemia/lymphoma.** *Clin Cancer Res* 2010, **16**:1520–1531.
30. Yamano Y, Araya N, Sato T, *et al*: **Abnormally high levels of virus-infected IFN-gamma+ CCR4+ CD4+ CD25+ T cells in a retrovirus-associated neuroinflammatory disorder.** *PLoS One* 2009, **4**:e6517.
31. Souquiere S, Mouinga-Ondeme A, Makuwa M, *et al*: **T-cell tropism of simian T-cell leukaemia virus type 1 and cytokine profiles in relation to proviral load and immunological changes during chronic infection of naturally infected mandrills (Mandrillus sphinx).** *J Med Primatol* 2009, **38**:279–289.
32. Stevens HP, Holterman L, Haaksma AG, Jonker M, Heeney JL: **Lymphoproliferative disorders developing after transplantation and their relation to simian T-cell leukemia virus infection.** *Transpl Int* 1992, **5**(Suppl 1):S450–S453.
33. Akari H, Ono F, Sakakibara I, *et al*: **Simian T cell leukemia virus type I-induced malignant adult T cell leukemia-like disease in a naturally infected African green monkey: implication of CD8+ T cell leukemia.** *AIDS Res Hum Retroviruses* 1998, **14**:367–371.
34. McCarthy TJ, Kennedy JL, Blakeslee JR, Bennett BT: **Spontaneous malignant lymphoma and leukemia in a simian T-lymphotropic virus type I (STLV-I) antibody positive olive baboon.** *Lab Anim Sci* 1990, **40**:79–81.
35. Sakakibara I, Sugimoto Y, Sasagawa A, *et al*: **Spontaneous malignant lymphoma in an African green monkey naturally infected with simian T-lymphotropic virus (STLV).** *J Med Primatol* 1986, **15**:311–318.
36. Afonso PV, Mekaouche M, Mortreux F, *et al*: **Highly active antiretroviral treatment against STLV-1 infection combining reverse transcriptase and HDAC inhibitors.** *Blood* 2010, **116**:3802–3808.
37. Zhao T, Yasunaga J, Satou Y, *et al*: **Human T-cell leukemia virus type 1 bZIP factor selectively suppresses the classical pathway of NF-kappaB.** *Blood* 2009, **113**:2755–2764.
38. Basbous J, Arpin C, Gaudray G, Piechaczyk M, Devaux C, Mesnard JM: **The HBZ factor of human T-cell leukemia virus type I dimerizes with transcription factors JunB and c-Jun and modulates their transcriptional activity.** *J Biol Chem* 2003, **278**:43620–43627.
39. Clerc I, Polakowski N, Andre-Arpin C, *et al*: **An interaction between the human T cell leukemia virus type 1 basic leucine zipper factor (HBZ) and the KIX domain of p300/CBP contributes to the down-regulation of tax-dependent viral transcription by HBZ.** *J Biol Chem* 2008, **283**:23903–23913.
40. Lairmore MD, Lerche NW, Schultz KT, *et al*: **SIV, STLV-I and type D retrovirus antibodies in captive rhesus macaques and immunoblot**

reactivity to SIV p27 in human and rhesus monkey sera. *AIDS Res Hum Retroviruses* 1990, 6:1233–1238.
41. Miyoshi I, Fujishita M, Taguchi H, Matsubayashi K, Miwa N, Tanioka Y: Natural infection in non-human primates with adult T-cell leukemia virus or a closely related agent. *Int J Cancer* 1983, 32:333–336.
42. Miyoshi I, Yoshimoto S, Fujishita M, *et al*: Natural adult T-cell leukemia virus infection in Japanese monkeys. *Lancet* 1982, 2:658.
43. Takemura T, Yamashita M, Shimada MK, *et al*: High prevalence of simian T-lymphotropic virus type L in wild ethiopian baboons. *J Virol* 2002, 76:1642–1648.
44. Graves LE, Hennessy A, Sunderland NS, Heffernan SJ, Thomson SE: Incidence of lymphoma in a captive-bred colony of hamadryas baboons (Papio hamadryas). *Aust Vet J* 2009, 87:238–243.
45. Hubbard GB, Mone JP, Allan JS, *et al*: Spontaneously generated non-Hodgkin's lymphoma in twenty-seven simian T-cell leukemia virus type 1 antibody-positive baboons (Papio species). *Lab Anim Sci* 1993, 43:301–309.
46. Yamamoto K, Utsunomiya A, Tobinai K, *et al*: Phase I study of KW-0761, a defucosylated humanized anti-CCR4 antibody, in relapsed patients with adult T-cell leukemia-lymphoma and peripheral T-cell lymphoma. *J Clin Oncol* 2010, 28:1591–1598.
47. Yasunaga J, Sakai T, Nosaka K, *et al*: Impaired production of naive T lymphocytes in human T-cell leukemia virus type I-infected individuals: its implications in the immunodeficient state. *Blood* 2001, 97:3177–3183.
48. Miyoshi I, Yoshimoto S, Fujishita M, *et al*: Isolation in culture of a type C virus from a Japanese monkey seropositive to adult T-cell leukemia-associated antigens. *Gann* 1983, 74:323–326.
49. Yanagawa S, Lee JS, Matsuda Y, Ishimoto A: Biochemical characterization of the Drosophila axin protein. *FEBS Lett* 2000, 474:189–194.
50. Fujisawa J, Toita M, Yoshimura T, Yoshida M: The indirect association of human T-cell leukemia virus tax protein with DNA results in transcriptional activation. *J Virol* 1991, 65:4525–4528.
51. Sugata K, Satou Y, Yasunaga J, *et al*: HTLV-1 bZIP factor impairs cell-mediated immunity by suppressing production of Th1 cytokines. *Blood* 2012, 119:434–444.
52. Satou Y, Utsunomiya A, Tanabe J, Nakagawa M, Nosaka K, Matsuoka M: HTLV-1 modulates the frequency and phenotype of FoxP3+CD4+ T cells in virus-infected individuals. *Retrovirology* 2012, 9:46.
53. Li H, Durbin R: Fast and accurate short read alignment with Burrows-Wheeler transform. *Bioinformatics* 2009, 25:1754–1760.

doi:10.1186/1742-4690-10-118
**Cite this article as:** Miura *et al.*: Characterization of simian T-cell leukemia virus type 1 in naturally infected Japanese macaques as a model of HTLV-1 infection. *Retrovirology* 2013 10:118.

ELSEVIER

Institut Pasteur

Microbes and Infection 15 (2013) 319–328

www.elsevier.com/locate/micinf

Original article

# Systemic biological analysis of the mutations in two distinct HIV-1mt genomes occurred during replication in macaque cells

Masako Nomaguchi [a], Naoya Doi [a], Sachi Fujiwara [a], Akatsuki Saito [b], Hirofumi Akari [b], Emi E. Nakayama [c], Tatsuo Shioda [c], Masaru Yokoyama [d], Hironori Sato [d], Akio Adachi [a,*]

[a] *Department of Microbiology, Institute of Health Biosciences, The University of Tokushima Graduate School, 3-18-15 Kuramoto, Tokushima 770-8503, Japan*
[b] *Center for Human Evolution Modeling Research, Primate Research Institute, Kyoto University, Aichi, Japan*
[c] *Department of Viral Infections, Research Institute for Microbial Diseases, Osaka University, Osaka, Japan*
[d] *Laboratory of Viral Genomics, Pathogen Genomics Center, National Institute of Infectious Diseases, Tokyo, Japan*

Received 17 December 2012; accepted 24 January 2013
Available online 4 February 2013

**Abstract**

Fundamental property of viruses is to rapidly adapt themselves under changing conditions of virus replication. Using HIV-1 derivatives that poorly replicate in macaque cells as model viruses, we studied here mechanisms for promoting viral replication in non-natural host cells. We found that the HIV-1s could evolve to grow better in both macaque and human cells by the continuous culture in macaque lymphocyte cell lines. Notably, only several mutations at defined sites of the Pol-integrase and/or the Env-gp120 reproducibly appeared in repeated adaptation experiments and were sufficient to cause the phenotypic change. Meanwhile, no amino acid changes to enhance viral replication in macaque cells were found in interaction sites for the known anti-retroviral proteins. These findings disclose a hitherto unappreciated evolutionary pathway to augment HIV-1 replication in primate cells, where tuning of viral interactions with positive rather than negative factors for replication can play a dominant role.


*Keywords:* HIV-1; HIV-1mt; Pol-IN; Env-gp120; Adaptive mutation; Macaque cells

## 1. Introduction

Viruses evolve extremely rapidly under the changing conditions of virus replication. HIV-1 is no exception. HIV-1 possesses high adaptation potential due to the ability to acquire sequence alterations through high mutation rate of reverse transcriptase (RT) and recombination of viral genomes [1,2]. Change of viral properties by genetic alterations leads to resistance to antiviral drugs, escape from host immune system, and adaptation to new hosts upon transmission [3–6]. Experimental approaches that analyze the genomic change and evolution of viruses are commonly used effective measures to know how viruses adapt themselves under a certain selective pressure. Such studies, however, usually have focused on genetic changes in a limited and selected region of viral genomes or sequence variations in a specified mass of virus.

HIV-1 does not replicate in most animal species including rodents and macaques. Inhibition of HIV-1 replication in macaque cells, at least in part, is mediated by host restriction factors such as APOBEC3 proteins, cyclophilin A (CypA), TRIM5α/TRIMCyp (TRIM5 proteins), and tetherin (for review, refer to references [7–10]). Encounters with pathogenic viruses impose selective pressure on restriction factors, and influence their antiviral specificity [11–13]. Even though human cells also have orthologs of these factors, HIV-1 evades their restriction and replicates well in humans. This suggests that both viruses and host cells co-evolve under the mutual selective pressure. Thus, evolution of viruses is determined by adaptation potential of viruses and their interaction with host cells.

* Corresponding author. Tel.: +81 88 633 7078; fax: +81 88 633 7080.
*E-mail address:* adachi@basic.med.tokushima-u.ac.jp (A. Adachi).

1286-4579/$ - see front matter © 2013 Institut Pasteur. Published by Elsevier Masson SAS. All rights reserved.
http://dx.doi.org/10.1016/j.micinf.2013.01.005

Prototype macaque cell-tropic HIV-1 (pHIV-1mt), NL-DT5R (5R; X4-tropic) and NL-DT562 (562; R5-tropic), carry a small portion of *gag* gene and an entire *vif* gene from SIVmac239 (Fig. 1). These viruses are insufficiently infectious for macaque cells by their partial resistance to CypA/TRIM5 proteins and evasion from APOBEC3G/F restriction, and their replication potentials were significantly lower than that of pathogenic SIVmac239 [14–16]. These results indicate that macaque cells still impose strong restrictive pressure on pHIV-1mt replication. Therefore, clones 5R and 562 are suitable materials to analyze what genetic changes they would acquire and how they would adapt themselves to environments within macaque cells. As experimental approach to do this, we have performed virus adaptation experiments by the long-term culture of 5R- or 562-infected macaque cells, and successfully obtained adapted viruses with enhanced growth ability [17]. In this study, we inquired into the biological relevance of mutations that appeared in the genomes of adapted viral clones by investigating thoroughly the effect of mutations on viral growth. Although a number of genetic substitutions were found in the genomes of adapted viruses, mutations in *pol*-integrase (IN) and *env*-gp120 only were found to be responsible for enhancement of viral replication. Extensive and repeated virus adaptation experiments revealed that viral clones with augmented growth potential are characterized by acquisition of adaptive mutations in *pol*-IN and in *env*-gp120. Our results suggest that pHIV-1mt evolves in a certain adaptation pathway under the restrictive and uniform environments imposed by macaque cells, and that genetic alterations do not always have biological significance for escaping selective pressure, supporting Kimura's neutral theory of molecular evolution [18].

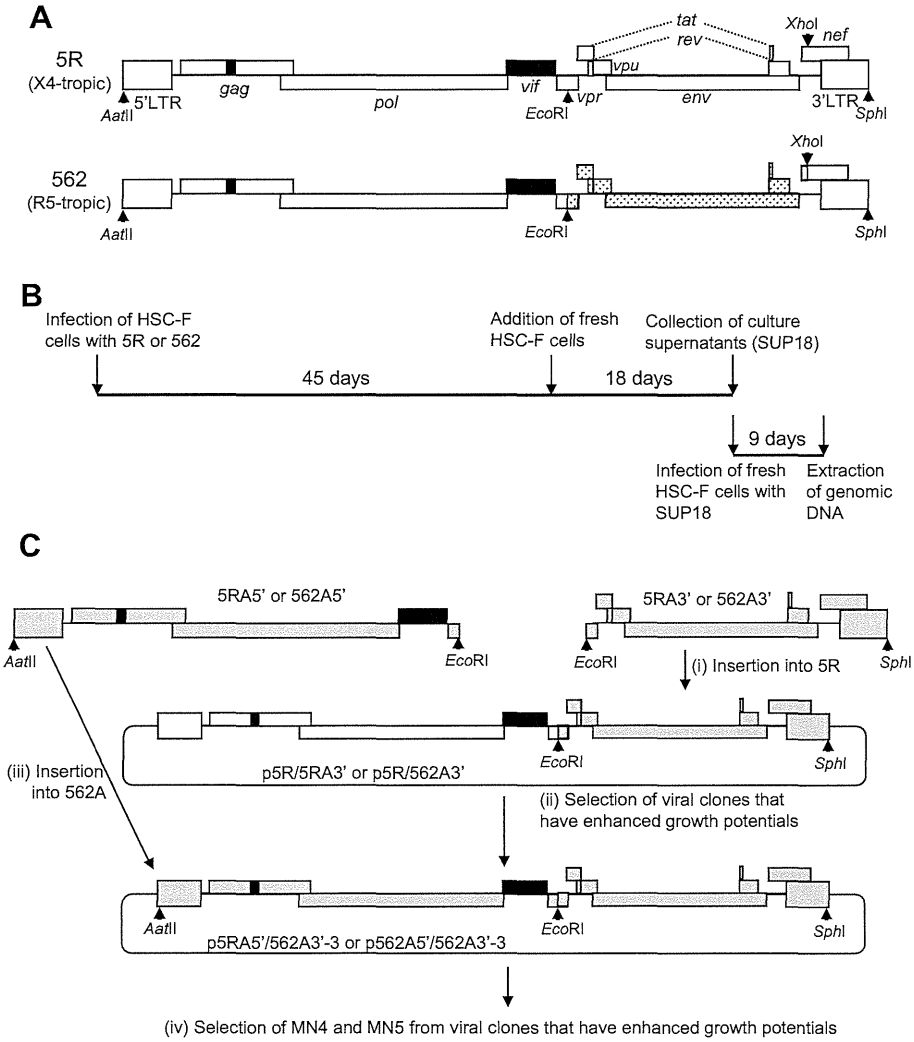


Fig. 1. Molecular cloning of viral genomes from macaque cell-adapted viruses. (A) Genome structure of 5R and 562 [14,16]. Sequence from NF462 [32] is shown by dotted areas. Black areas show the regions derived from SIVmac239. (B) Schedule of virus adaptation and the harvest of adapted viruses [17]. Genomic DNA prepared from infected cells for molecular cloning is indicated. (C) Generation and selection of proviral clones from adapted 5R and 562 viruses. The procedure starts with (i) and ends with (iv). For details, see Materials and methods. PCR-amplified fragments derived from adapted 5R (5RA) or adapted 562 (562A) are shown by gray areas. White and black areas indicate the region from 5R.

## 2. Materials and methods

### 2.1. Cells

A human monolayer cell line 293T [19] was cultured in Eagle's MEM supplemented with 10% heat-inactivated FBS (hiFBS). A cynomolgus macaque (CyM) lymphocyte cell line HSC-F [20] and a rhesus monkey (RhM) lymphocyte cell line HSR5.4S1 [21] were maintained in RPMI1640 containing 10% hiFBS (for HSR5.4S1, 50 units/mL of IL-2 (AbD Serotec) were added). Human MT4/CCR5 cells (MT4 cells stably expressing CCR5) were maintained RPMI1640 containing 10% hiFBS and 200 μg/mL of hygromycin B (Sigma–Aldrich).

### 2.2. Transfection, RT assays and infection

Virus stocks were prepared by transfection of 293T cells with viral clones using the calcium phosphate co-precipitation method [22]. On day 2 post-transfection, culture supernatants were collected and stored at −80 °C until use. Virion-associated RT activity was measured as described previously [23]. HSC-F cells were infected with an equal amount of virus preparations in the presence of IL-2. For infection of MT4/CCR5 cells, the spinoculation method [24] was used. Virus replication was monitored by RT activity in the culture supernatants, and viral growth potentials were evaluated by the peak day of virus production or by the level of virus production on the peak day.

### 2.3. Plasmid DNAs

Construction of pHIV-1mt clones designated 5R and 562 has been previously described [14,16]. Proviral clones derived from adapted viruses were generated by PCR as described previously [14]. Two rounds of adaptation experiments independently performed are outlined in Figs. 1–4, and their details are described below. Introduction of genetic substitutions was performed by the QuickChange site-directed mutagenesis kit (Agilent Technologies).

### 2.4. First adaptation experiment

As indicated in Fig. 1, to construct molecular clones of adapted viruses from 5R and 562, CyM HSC-F cells were infected with the culture supernatants collected from long-term cultures. On day 9 post-infection, genomic DNA was extracted from cells, and integrated proviruses were amplified as two overlapping fragments by PCR as described previously [14]. To generate molecular clones that exhibit phenotypes of adapted viruses, we first introduced 3′ half genomes (*Eco*RI site in Vpr to *Sph*I site at 3′ end of the genome) from adapted 5R (5RA) and 562 (562A) viruses into 5R, and the resultant constructs were designated p5R/5RA3′ and p5R/562A3′, respectively. Virus stocks were prepared from 293T cells transfected with p5R/5RA3′ or p5R/562A3′, and inoculated into HSC-F cells. Virus replication was monitored by RT activity released into the culture supernatant. A molecular clone that grows best was selected for 5RA and 562A (p5R/5RA3′-14 and p5R/562A3′-3, respectively). Then, 5′ half genomes (*Aat*II site at the 5′ end of the genome to *Eco*RI site in Vpr) of adapted viruses (5RA5′ and 562A5′) were introduced into the selected clone (p5R/562A3′-3), and the resultant constructs were designated p5RA5′/562A3′-3 and p562A5′/562A3′-3, respectively. Proviral clones with the best replication potential were selected as described above. Finally, proviral clones that have a full-length viral genome derived from adapted 5R and 562 viruses were constructed, and designated MN4 and MN5, respectively (see Fig. 2 for their genome structures).

### 2.5. Second adaptation experiment

As indicated in Fig. 4, HSC-F ($1 \times 10^6$) and RhM HSR5.4S1 cells ($3 \times 10^6$) were infected with 5R or 562 viruses prepared from transfected 293T cells to obtain adapted viruses. Half of the culture medium (5 mL) was replaced every 3 days. Fresh HSC-F ($1 \times 10^6$) and HSR5.4S1 cells ($3 \times 10^6$) were added in each long-term culture on day 28 post-infection. Half of the culture medium (5 mL) was replaced every 3 days, and harvested supernatants were stored at −80 °C. HSC-F cells were infected with supernatants collected on day 33 post-infection from 5R- or 562-infected HSC-F long-term cultures. On day 9 and 12 post-infection, genomic DNA was extracted from infected cells. For HSR5.4S1 cultures, supernatants collected from 5R- and 562-infected cultures on day 39 and 42 post-infection, respectively, were inoculated into fresh HSR5.4S1 cells. On day 8 and 11 post-infection, genomic DNA was extracted from infected cultures. Amplification of integrated proviruses from genomic DNA and construction of proviral clones were carried out as described above. Viruses prepared from 293T cells transfected with these proviral clones were inoculated into HSC-F and HSR5.4S1 cells depending on which cells were used for long-term culture. Selection of viral clones with enhanced replication capability was carried out as described above.

## 3. Results

### 3.1. Mutations in Pol-IN or Env-gp120 are important for enhancement of pHIV-1mt replication in macaque cells

We previously reported that adapted viruses with enhanced growth potential emerged in prolonged cultures of 5R- or 562-infected macaque (CyM) cells [17]. Genomes of adapted viruses should have some genetic changes to augment their growth ability, and adapted viruses were expected to exist as a mass of viruses with distinct replication potential. To identify an adaptive mutation responsible for enhanced growth potential, it is necessary to construct proviral clones that exhibit a better-growing phenotype. Experimental details for construction are shown in Fig. 1. Of 72 proviral clones constructed, some of them (9 clones) did not produce virions in transfected 293T cells as determined by virion-associated RT activity or were not infectious for a CyM lymphocyte cell line HSC-F as well (16 clones). Finally, we have obtained molecular clones

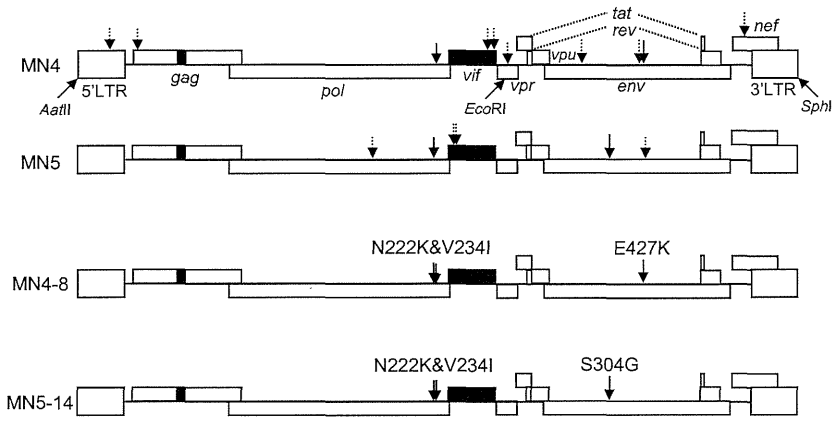


| Virus | Genomes from adapted virus | Nucleotide change | Region | Amino acid change in the region |
|---|---|---|---|---|
| MN4 | 5' half | t453c | LTR | None |
| (derived from adapted 5R) | (MN4-5') | g823a | Matrix | E12K |
| | | **g4923a** | **Pol-IN** | **V234I** |
| | | g5611a | Vif | R171K |
| | | g5693a | Vif | None |
| | 3' half | g5944a | Vpr | None |
| | (MN4-3') | g6915a | Env-gp120 (V2) | None |
| | | g7606a | Env-gp120 (V4) | E401K |
| | | **g7684a** | **Env-gp120 (C4)** | **E427K** |
| | | g9191a | Nef | V74I |
| MN5 | 5' half | a4049c | Reverse transcriptase | None |
| (derived from adapted 562) | (MN5-5') | **t4889a** | **Pol-IN** | **N222K** |
| | | g5156a | Vif | None |
| | | t5195a | Vif | None |
| | 3' half | **a7318g** | **Env-gp120 (V3 loop)** | **S304G** |
| | (MN5-3') | c7812t | Env-gp120 (C5) | None |

Fig. 2. Various mutations found in the first adaptation experiment. (Upper) Proviral genome structures of MN4, MN5, and their derivatives. Black areas show the regions derived from SIVmac239. Broken arrows show mutations that appeared during viral adaptation. Solid arrows indicate adaptive mutations in Pol-IN and Env-gp120 that enhance viral growth (Fig. 3). Out of the mutations present in MN4 and MN5, clones MN4-8 and MN5-14 carry the adaptive (growth-enhancing) mutations only. (Lower) Mutations associated with adaptation of 5R and 562 viruses to HSC-F cells. Bold letters show adaptive mutations that are responsible for enhancement of viral replication in cells. 5′ half indicates a fragment from *Aat*II at the 5′ end to *Eco*RI in *vpr* of the viral genome. 3′ half indicates a fragment from *Eco*RI in *vpr* to *Sph*I at the 3′ end of the viral genome.

MN4 and MN5 from adapted 5R and 562 viruses, respectively (Fig. 2).

To identify genetic changes acquired in genomes during virus adaptation, the entire genomes of MN4 and MN5 were sequenced. As shown in Fig. 2, MN4 and MN5 contained ten and six nucleotide substitutions, respectively. To examine the effect of these mutations on viral replication, each mutation was introduced into parental clones 5R and 562 as follows: (i) mutations in MN4 were introduced into 5R; (ii) mutations in 5′ half of MN5 genome were introduced into 5R (5′ half of 562 genome is identical to that of 5R (see Fig. 1A)); (iii) mutations in 3′ half of MN5 genome were introduced into 562. To construct positive control clones for viral growth (Fig. 3), we inserted a half of MN4 and MN5 genomes into the corresponding regions of 5R to generate full-length clones MN4-5′/5R, 5R/MN4-3′, MN5-5′/5R, and 5R/MN5-3′ (Fig. 2). Viruses were then prepared from 293T cells transfected with parental clones, positive controls, or test clones carrying each mutation, and inoculated into HSC-F cells (Fig. 3). MN4-5′ contains five genetic mutations (Fig. 2). Of the five clones examined, only the 5R carrying g4923a (V234I in IN) exhibited a similar growth kinetics to MN4-5′/5R (Fig. 3A). Growth kinetics of 5R carrying the other mutations were similar or slower relative to the parental clone 5R (Fig. 3A). MN4-3′ and MN5-5′ carry five and four nucleotide substitutions, respectively (Fig. 2). A clone that exhibits similar growth kinetics to 5R/MN4-3′ was 5R carrying g7684a

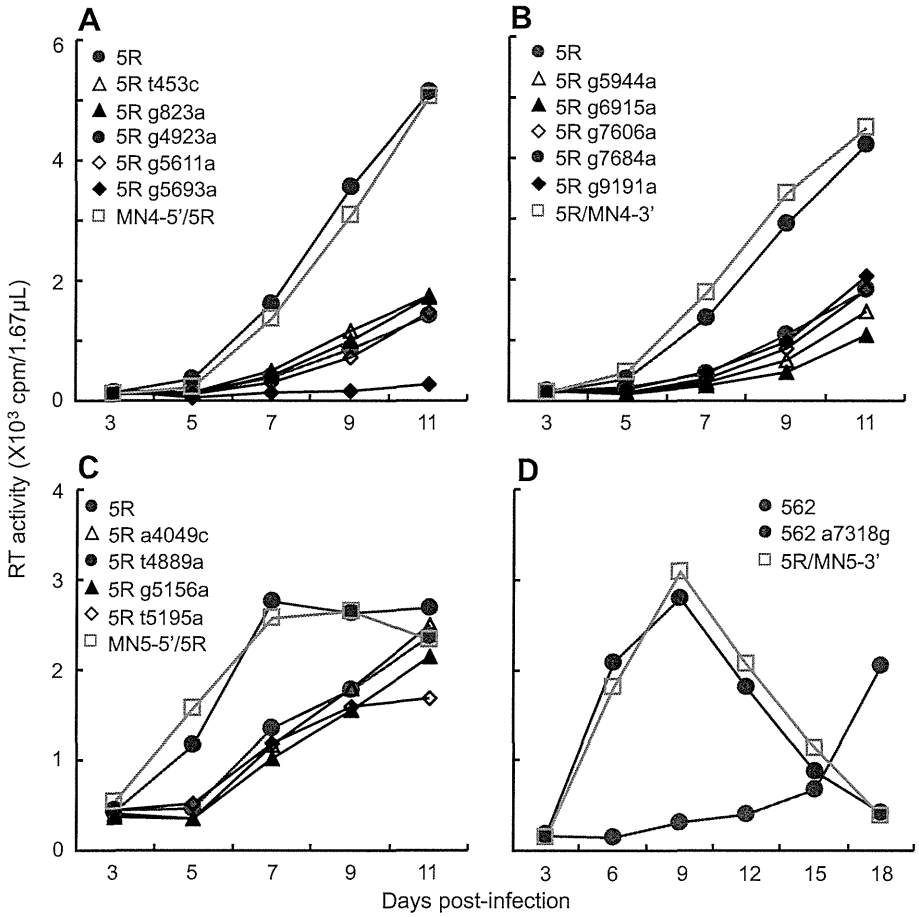


Fig. 3. Effect of individual mutations found in MN4 and MN5 on viral replication in HSC-F cells. Virus samples were prepared from 293T cells transfected with the indicated proviral clones, and inoculated into HSC-F cells ($10^6$) with an equal amount of viruses (A; $1.6 \times 10^7$ RT units, B; $8.5 \times 10^6$ RT units, C; $3.9 \times 10^7$ RT units, and D; $1.2 \times 10^7$ RT units). Proviral clones, MN4-5′/5R, 5R/MN4-3′, MN5-5′/5R, and 5R/MN5-3′, carry 5′ or 3′ half genomes of MN4 or MN5 in the context of 5R genome (Fig. 2). These clones served as positive controls. Virus replication was monitored by RT activity released into the culture supernatants.

(E427K in gp120) (Fig. 3B). 5R carrying t4889a (N222K in IN) showed a similar growth property with MN5-5′/5R (Fig. 3C). Two mutations (non-synonymous and synonymous) were found in MN5-3′ (Fig. 2), but only the non-synonymous mutation (a7318g, S304G in gp120) was tested. The viral clone 562 a7318g showed similar growth kinetics to those of 5R/MN5-3′ (Fig. 3D). In total, the growth-enhancing mutations were found only in *pol*-IN (V234I in 5R and N222K in 562) and *env*-gp120 (E427K in 5R and S304G in 562) regions despite the presence of mutations in the other regions.

### *3.2. Adaptive mutations in Pol-IN and 562 Env-gp120 are critical for augmentation of pHIV-1mt replication*

Growth potential of both MN4 and MN5 obtained from adaptation of two distinct viruses was augmented by mutations in Pol-IN and Env-gp120 (Figs. 2 and 3). To clarify the requirements of adaptive mutations in these regions for enhancement of viral replication, we repeated the virus adaptation experiment (Fig. 4). Because it has been suggested that cellular environment is different between cell lines and affects outcome of virus adaptation [25], we used two distinct viruses (5R and 562) and two different macaque lymphocyte cell lines (CyM HSC-F and RhM HSR5.4S1) in this experiment. During long-term cultures of HSC-F and HSR5.4S1 cells infected with 5R or 562, adapted viruses emerged as judged by the growth property of viruses produced in the culture supernatants as previously described [17]. A number of proviral clones derived from adapted viruses were constructed similarly as above, and test viruses were prepared from transfected 293T cells. Viruses were then inoculated into HSC-F or HSR5.4S1 cells depending on which cells were used for adaptation. We selected proviral clones that show clearly enhanced viral replication in macaque cells, and sequenced their entire genomes. As shown in Fig. 4, of viral clones that bear 5′ half of genomes from adapted 5R, we selected four clones from HSC-F cells and one clone from HSR5.4S1 cells. All of them carried a genetic mutation in Pol-IN (D229E or F223Y) that enhances viral growth potential (Fig. 4B, note the peak day of virus production). Four adaptive mutations identified in Pol-IN (N222K, F223Y, D229E and V234I) were located in a narrow region of IN C-terminal domain (IN-CTD). On the other hand, none of viral clones carrying 3′ half of genomes from adapted 5R exhibited augmentation of viral

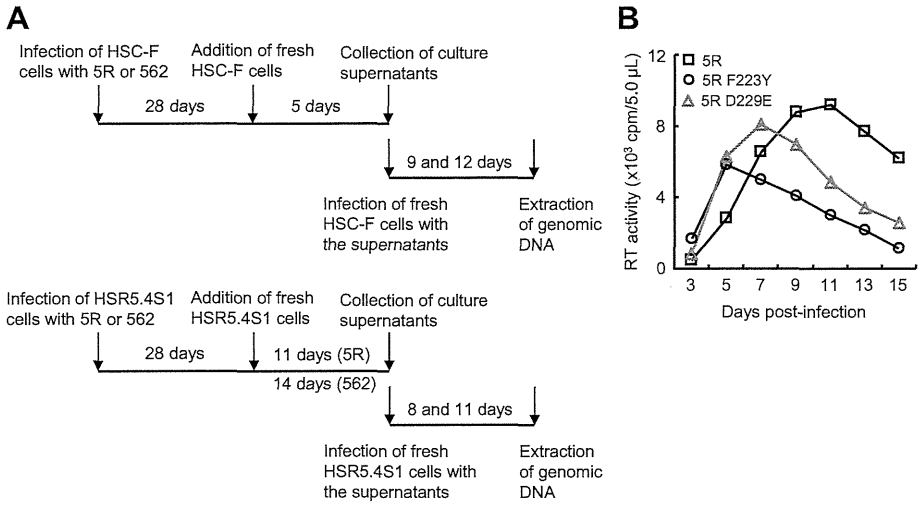


C

| Virus/Macaque cells used for long-term culture | Half genome derived from adapted viruses | Number of clones examined for growth kinetics | Number of clones with enhanced viral growth | Adaptive mutations in IN-CTD and Env-gp120 |
|---|---|---|---|---|
| 5R/HSC-F | 5' | 39 | 4 | IN-CTD D229E (4) |
| | 3' | 43 | 0 | NA |
| 5R/HSR5.4S1 | 5' | 24 | 1 | IN-CTD F223Y (1) |
| | 3' | 62 | 0 | NA |
| 562/HSC-F | 5' | 41 | 1 | IN-CTD N222K (1) |
| | 3' | 16 | 13 | V3 S304G (8)<br>V1 G150R (2)<br>C1 L124F (1)<br>V1 N132K (1)<br>V3 I307V (1) |
| 562/HSR5.4S1 | 5' | 27 | 0 | NA |
| | 3' | 32 | 20 | V3 S304G (9)<br>V2 F174L (7)<br>V1 L124F (1)<br>V2 P181T (1)<br>V3 G308E (1)<br>V3 G310R (1) |

Fig. 4. Various adaptive (growth-enhancing) mutations found in the second adaptation experiment. (A) Generation of molecular clones from adapted 5R and 562 viruses. Schedule of virus adaptation and the harvest of adapted viruses are shown. Cellular genomic DNA preparations for molecular cloning of viruses are indicated. For details, see Materials and methods. (B) Growth kinetics of Pol-IN mutants in HSC-F cells. Virus samples ($3.5 \times 10^6$ RT units) were prepared from 293T cells transfected with the indicated proviral clones, and inoculated into CyM HSC-F ($10^6$). Virus replication was monitored by RT activity released into the culture supernatants. (C) Frequency of adaptive mutations in IN-CTD and Env-gp120. Number in parentheses refers to the number of clones carrying the indicated mutation. In total, all viral clones with enhanced growth potential were found to have adaptive mutations in IN-CTD or Env-gp120. NA, not applicable.

replication. This may imply that 5R has been already better adapted to HSC-F cells, since 5R has acquired mutations in *env* and LTR by virus adaptation within the cells [14]. In viral clones bearing 5′ half genome from adapted 562, one selected clone carried the same N222K mutation in IN-CTD as MN5. Enhanced growth potentials were noted for many clones that carry 3′ half genome from adapted 562. Around half of the selected clones carried S304G in Env-gp120 V3 loop, and the rest of clones carried adaptive (growth-enhancing) mutations in the C1, V1, V2, or V3 region of Env-gp120. Similar results with those in HSC-F cells were obtained in HSR5.4S1 cells (data not shown). The results described above indicate that adaptive mutations in IN-CTD and 562 Env-gp120 are critical for enhancement of viral growth potential in macaque cells.

### *3.3. Introduction of either single or double adaptive IN-CTD mutations (N222K and V234I) enhances viral growth both in macaque and human cells*

Replication of two distinct pHIV-1mt was augmented by acquiring N222K or V234I in IN-CTD during virus adaptation in macaque cells (Figs. 2 and 3). To examine whether these adaptive mutations have an additive effect on viral replication, we constructed 5R carrying single (designated 5R N222K and 5R V234I) or double (designated 5R NKVI) mutations. We were also interested in determining the effect of the mutations on viral growth in human cells. Viruses prepared from transfected 293T cells were inoculated into HSC-F and human MT4/CCR5 cells. As shown in Fig. 5A, 5R NKVI exhibited similar growth kinetics in macaque HSC-

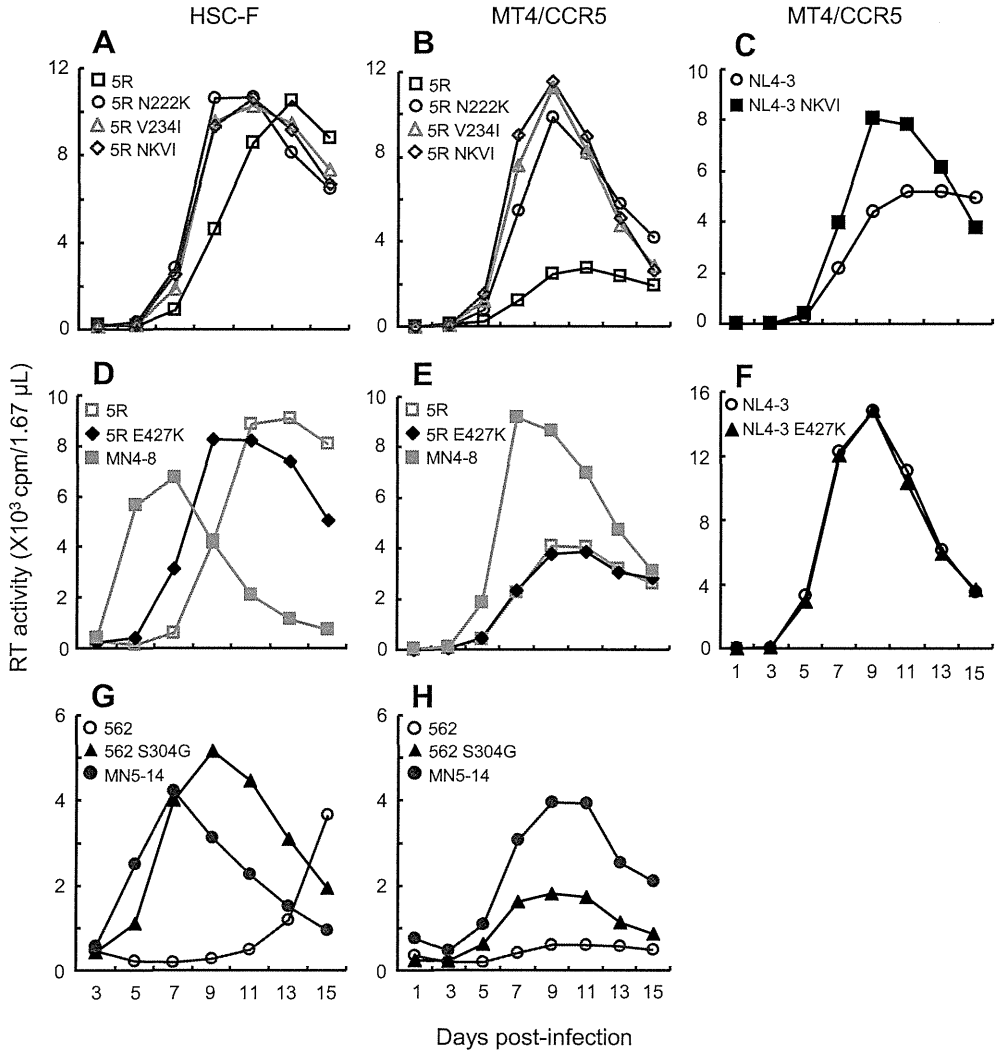


Fig. 5. Effect of adaptive mutations on viral replication. Growth kinetics in the indicated cell lines of various mutant viruses are presented. Virus samples were prepared from 293T cells transfected with the indicated proviral clones, and inoculated into CyM HSC-F ($10^6$) or spinoculated into human MT4/CCR5 ($10^6$) cells. Input viral amounts used were $1.0 \times 10^7$ RT units, $1.0 \times 10^6$ RT units, $1.1 \times 10^5$ RT units, $1.2 \times 10^7$ RT units, $1.0 \times 10^6$ RT units, $1.3 \times 10^5$ RT units, $1.2 \times 10^7$ RT units and $2.8 \times 10^7$ RT units for panels A, B, C, D, E, F, G and H, respectively. Virus replication was monitored by RT activity released into the culture supernatants. (A and B) Growth kinetics of 5R carrying single or double adaptive mutations in IN-CTD. 5R NKVI contains both N222K and V234I mutations. 5R served as a control. (C and F) Growth kinetics of NL4-3 viruses bearing IN NKVI (N222K and V234I) or Env E427K mutation. NL4-3 served as control. (D, E, G and H) Growth kinetics of various viruses carrying adaptive mutations. 5R and 562 served as controls.

F cells to those of 5R N222K and 5R V234I, and all these viruses grew better than 5R. Essentially the same results were obtained in human MT4/CCR5 cells (Fig. 5B). To determine whether the viral growth enhancement by adaptive mutations in IN-CTD is specific to pHIV-1mt, the mutational effect in the context of a standard HIV-1 clone NL4-3 was examined in MT4/CCR5 cells. As is clear in Fig. 5C, the adaptive mutations in IN-CTD also enhanced NL4-3 replication. Unexpectedly, we found that the four adaptive mutations in IN-CTD (Figs. 2 and 4) augment virion production independently of the IN authentic function (manuscript in preparation). In sum, these results show that adaptive mutations in IN-CTD augment growth potential of HIV-1, and that this effect is neither host-cell species-specific nor viral clone-specific.

### *3.4. E427K in 5R Env-gp120 promotes viral growth specifically in macaque cells, whereas enhancement of viral growth by S304G in 562 Env-gp120 is observed both in macaque and human cells*

We constructed proviral clones that have both adaptive mutations in Pol-IN and Env-gp120 in anticipation of additive positive effects. Two mutations in Pol-IN (N222K and V234I) were introduced into clones 5R E427K and 562 S304G, which carry an adaptive mutation in Env-gp120, and designated MN4-8 and MN5-14, respectively (Fig. 2). Viruses prepared from transfected 293T cells were inoculated into HSC-F and MT4/CCR5 cells, and monitored for their growth kinetics (Fig. 5). 5R E427K exhibited rapid growth kinetics relative to 5R in HSC-F cells, but similar in MT4/CCR5 cells (Fig. 5D

and E). To confirm this result, E427K was introduced into NL4-3 Env, which is the origin of 5R Env. NL4-3 carrying E427K showed similar growth kinetics to those of NL4-3 in MT4/CCR5 cells (Fig. 5F). Quite in contrast, the replication of 562 S304G was accelerated compared to that of 562 both in human and macaque cells (Fig. 5G and H). These results indicate that the effect of E427K mutation is host cell species-specific, whereas S304G shows the species-independent positive effect. Notably, E427K and S304G mutations were found to increase viral binding efficiency to CD4 and affinity to CCR5, respectively (manuscript in preparation). Growth potential of MN4-8 and MN5-14 was further enhanced both in macaque and human cells relative to 5R E427K and 562 S304G, respectively (Fig. 5), showing that combination of adaptive mutations in IN-CTD and Env-gp120 has an additive effect on viral replication (note the peak day of virus production).

### *3.5. Enhancement of viral growth by adaptive Env-gp120 mutations is dependent on the env sequence context*

E427K in 5R and S304G in 562 were located in a distinct region within Env-gp120, C4 region and V3 loop, respectively. Alignment of Env-gp120 amino acid sequence of 5R and 562 indicated that the corresponding sites of E427K and S304G are E419K for 562 and S304G for 5R, respectively (Fig. 6A). Since functional relationship between C4 region and V3 loop for viral infection has been reported [26,27], we examined the effect of combination of adaptive mutations in these regions on viral growth. Proviral clones were generated by introducing S304G into 5R and 5R E427K (designated 5R S304G and 5R SGEK, respectively), and E419K into 562 and 562 S304G (designated 562 E419K and 562 SGEK, respectively). Viruses prepared from transfected 293T cells were inoculated into HSC-F cells, and monitored for their growth property. As shown in Fig. 6B and C, while enhancement of viral replication was again observed for 5R E427K and 562 S304G relative to 5R and 562, respectively, the growth of 5R S304G and 562 E419K was undetectable. Clones 5R SGEK and 562 SGEK somewhat restored their infectivity. These results show that the positive effect of adaptive mutations in Env-gp120 is sequence-specific. This is similar to the result in a previous report that the impact of one amino acid change within V3 loop on sensitivity to entry inhibitors is dependent on *env* context [28].

## 4. Discussion

In this study, we generated MN4 and MN5 clones with enhanced growth potential by virus adaptation in macaque cells. MN4 and MN5 have a number of nucleotide substitutions throughout their genomes (Fig. 2). Interestingly, only the mutations in IN-CTD and Env-gp120 were responsible for augmentation of viral replication (Figs. 2 and 3). In the second round of virus adaptation experiment using two distinct viruses and two different kinds of macaque cells, the mutations in IN-CTD and in 562 Env-gp120 were frequently found in the genomes of viral clones that exhibit rapid growth kinetics (Fig. 4). These results indicate that adaptive mutations in

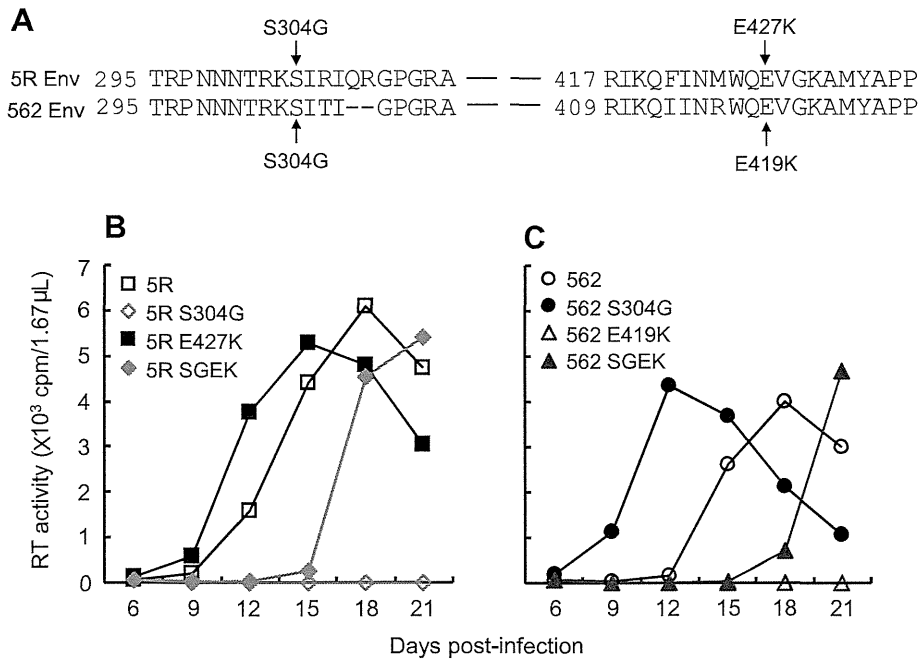


Fig. 6. Effect of combination of the adaptive mutations in Env-gp120 on viral replication. (A) Amino acid alignment of the regions close to adaptive mutations in 5R and 562. The corresponding sites to adaptive mutations in 5R and 562 are indicated. (B and C) Growth kinetics in HSC-F cells of 5R and 562 viruses carrying Env E419K/E427K and/or S304G mutation. Virus samples were prepared from 293T cells transfected with the indicated proviral clones, and inoculated into HSC-F cells ($10^6$) with an equal amount of viruses ($1.0 \times 10^7$ RT units). 5R SGEK and 562 SGEK carry both S304G and E419K/E427K mutations. 5R and 562 served as controls. Virus replication was monitored by RT activity released into the culture supernatants.

a narrow region of IN-CTD and in Env-gp120 are critical for growth-adaptation of pHIV-1mt in macaque cells. These results also suggest that pHIV-1mt may evolve in a certain direction to enhance their replication under uniform and strong restrictive environment in macaque cells. Notably, of the adaptive mutations examined, almost all were effective in both macaque and human cells with respect to promoting virus replication (Fig. 5).

In virus adaptation experiments, we obtained numerous proviral clones carrying the mutations in IN-CTD or S304G in 562, which exhibit enhanced growth potential (Figs. 2 and 4). Because genetic changes found in the other regions were different, the mutations came from different virus clones. Reason for the observed high frequency of adaptive IN-CTD and S304G mutations is presently unclear. Viruses may be apt to acquire the mutations in IN-CTD and Env-gp120 regions during adaptation by unknown mechanism. Alternatively, the rapid replication of mutant clones expanded the mutations in a mass of viruses, and resulted in their frequent selection. On the other hand, mutations in IN-CTD and S304G in 562 gp120 enhanced viral growth both in macaque and human cells (Fig. 5). These results indicate that the mutations are not relevant to evasion from the restriction factors responsible or critical for species-tropism. In fact, genetic alterations that influence viral replication were not found in *vif*, *gag*-CA, and *vpu*, which target APOBEC3G/F, CypA/TRIM5 proteins, and tetherin, respectively (Figs. 2 and 4). In this regard, it is interesting to note that replication efficiency of pHIV-1mt (5R and 562) is quite low in macaque cells [14,15]. Strong restriction of replication imposed by macaque cells may serve as a selective pressure on viruses during adaptation. Under this pressure, pHIV-1mt would have evolved to enhance growth ability itself, probably at a basal level, by acquiring the IN-CTD and gp120 mutations rather than to overcome the species barrier. HIV-1mt derivatives described in this report are still poorly infectious for CyM peripheral blood mononuclear cells (PBMCs) relative to the standard SIVmac and SHIV (chimera between SIVmac and HIV-1) clones. However, the enhancing effect of IN-CTD and Env-gp120 mutations was also observed in $CD8^+$ cell-depleted CyM PBMCs [29], confirming the results obtained in the cell lines. To further enhance growth potentials of HIV-1mt clones, it was found to be necessary to efficiently evade the species barrier [29,30]. Detailed functional and structural analyses of the mutations are required to elucidate the whole picture of the adaptive evolution described here. Studies in this direction are in progress in our laboratory.

In conclusion, we have demonstrated here that our adaptation system using virus-infected cells is a powerful tool to study virus replication and its underlying mechanism. We have readily and successfully identified the mutations, from mixtures of biologically insignificant and significant ones, that play a key role in viral replication, as also shown for SIVcpz (SIV isolated from chimpanzees) in human lymphoid tissue [31]. Since how viruses change their phenotypes is dependent on a power balance between viruses and cells, the combination of various primate lentiviruses (HIVs versus SIVs) and cells (human versus macaque) can produce different results upon adaptation. Information of adaptive mutations obtained from these experiments would be invaluable to learn and understand mechanisms for virus replication and evolution.

## Acknowledgments

We thank Ms. Kazuko Yoshida for editorial assistance. This study is supported by a grant from the Ministry of Health, Labour and Welfare of Japan (Research on HIV/AIDS project no. H23-003).

## References

[1] L.M. Mansky, H.M. Temin, Lower in vivo mutation rate of human immunodeficiency virus type 1 than that predicted from the fidelity of purified reverse transcriptase, J. Virol. 69 (1995) 5087–5094.
[2] D.N. Levy, G.M. Aldrovandi, O. Kutsch, G.M. Shaw, Dynamics of HIV-1 recombination in its natural target cells, Proc. Natl. Acad. Sci. U. S. A. 101 (2004) 4204–4209.
[3] J.M. Coffin, HIV population dynamics in vivo: implications for genetic variation, pathogenesis, and therapy, Science 267 (1995) 483–489.
[4] M.H. Malim, M. Emerman, HIV-1 sequence variation: drift, shift, and attenuation, Cell 104 (2001) 469–472.
[5] T. van Opijnen, B. Berkhout, The host environment drives HIV-1 fitness, Rev. Med. Virol. 15 (2005) 219–233.
[6] J.M. Carlson, Z.L. Brumme, HIV evolution in response to HLA-restricted CTL selection pressures: a population-based perspective, Microbes Infect. 10 (2008) 455–461.
[7] R.K. Holmes, M.H. Malim, K.N. Bishop, APOBEC-mediated viral restriction: not simply editing? Trends Biochem. Sci. 32 (2007) 118–128.
[8] J. Luban, Cyclophilin A, TRIM5, and resistance to human immunodeficiency virus type 1 infection, J. Virol. 81 (2007) 1054–1061.
[9] H. Huthoff, G.J. Towers, Restriction of retroviral replication by APOBEC3G/F and TRIM5alpha, Trends Microbiol. 16 (2008) 612–619.
[10] A. Tokarev, M. Skasko, K. Fitzpatrick, J. Guatelli, Antiviral activity of the interferon-induced cellular protein BST-2/tetherin, AIDS Res. Hum. Retroviruses 25 (2009) 1197–1210.
[11] S.L. Sawyer, M. Emerman, H.S. Malik, Ancient adaptive evolution of the primate antiviral DNA-editing enzyme APOBEC3G, PLoS Biol. 2 (2004) E275.
[12] S.L. Sawyer, L.I. Wu, M. Emerman, H.S. Malik, Positive selection of primate TRIM5alpha identifies a critical species-specific retroviral restriction domain, Proc. Natl. Acad. Sci. U. S. A. 102 (2005) 2832–2837.
[13] M.W. McNatt, T. Zang, T. Hatziioannou, M. Bartlett, I.B. Fofana, W.E. Johnson, S.J. Neil, P.D. Bieniasz, Species-specific activity of HIV-1 Vpu and positive selection of tetherin transmembrane domain variants, PLoS Pathog. 5 (2009) e1000300.
[14] K. Kamada, T. Igarashi, M.A. Martin, B. Khamsri, K. Hatcho, T. Yamashita, M. Fujita, T. Uchiyama, A. Adachi, Generation of HIV-1 derivatives that productively infect macaque monkey lymphoid cells, Proc. Natl. Acad. Sci. U. S. A. 103 (2006) 16959–16964.
[15] T. Igarashi, R. Iyengar, R.A. Byrum, A. Buckler-White, R.L. Dewar, C.E. Buckler, H.C. Lane, K. Kamada, A. Adachi, M.A. Martin, Human immunodeficiency virus type 1 derivative with 7% simian immunodeficiency virus genetic content is able to establish infections in pig-tailed macaques, J. Virol. 81 (2007) 11549–11552.
[16] T. Yamashita, N. Doi, A. Adachi, M. Nomaguchi, Growth ability in simian cells of monkey cell-tropic HIV-1 is greatly affected by downstream region of the vif gene, J. Med. Invest. 55 (2008) 236–240.
[17] M. Nomaguchi, N. Doi, K. Kamada, A. Adachi, Species barrier of HIV-1 and its jumping by virus engineering, Rev. Med. Virol. 18 (2008) 261–275.
[18] M. Kimura, Evolutionary rate at the molecular level, Nature 217 (1968) 624–626.

[19] J.S. Lebkowski, S. Clancy, M.P. Calos, Simian virus 40 replication in adenovirus-transformed human cells antagonizes gene expression, Nature 317 (1985) 169–171.
[20] H. Akari, T. Fukumori, S. Iida, A. Adachi, Induction of apoptosis in *Herpesvirus saimiri*-immortalized T lymphocytes by blocking interaction of CD28 with CD80/CD86, Biochem. Biophys. Res. Commun. 263 (1999) 352–356.
[21] N. Doi, S. Fujiwara, A. Adachi, M. Nomaguchi, Growth ability in various macaque cell lines of HIV-1 with simian cell-tropism, J. Med. Invest. 57 (2010) 284–292.
[22] A. Adachi, H.E. Gendelman, S. Koenig, T. Folks, R. Willey, A. Rabson, M.A. Martin, Production of acquired immunodeficiency syndrome-associated retrovirus in human and nonhuman cells transfected with an infectious molecular clone, J. Virol. 59 (1986) 284–291.
[23] R.L. Willey, D.H. Smith, L.A. Lasky, T.S. Theodore, P.L. Earl, B. Moss, D.J. Capon, M.A. Martin, In vitro mutagenesis identifies a region within the envelope gene of the human immunodeficiency virus that is critical for infectivity, J. Virol. 62 (1988) 139–147.
[24] U. O'Doherty, W.J. Swiggard, M.H. Malim, Human immunodeficiency virus type 1 spinoculation enhances infection through virus binding, J. Virol. 74 (2000) 10074–10080.
[25] T. van Opijnen, A. de Ronde, M.C. Boerlijst, B. Berkhout, Adaptation of HIV-1 depends on the host-cell environment, PLoS One 2 (2007) e271.
[26] A. Carrillo, L. Ratner, Human immunodeficiency virus type 1 tropism for T-lymphoid cell lines: role of the V3 loop and C4 envelope determinants, J. Virol. 70 (1996) 1301–1309.
[27] N.G. Hoffman, F. Seillier-Moiseiwitsch, J. Ahn, J.M. Walker, R. Swanstrom, Variability in the human immunodeficiency virus type 1 gp120 Env protein linked to phenotype-associated changes in the V3 loop, J. Virol. 76 (2002) 3852–3864.
[28] M.A. Lobritz, A.J. Marozsan, R.M. Troyer, E.J. Arts, Natural variation in the V3 crown of human immunodeficiency virus type 1 affects replicative fitness and entry inhibitor sensitivity, J. Virol. 81 (2007) 8258–8269.
[29] A. Saito, M. Nomaguchi, S. Iijima, A. Kuroishi, T. Yoshida, Y.J. Lee, T. Hayakawa, K. Kono, E.E. Nakayama, T. Shioda, Y. Yasutomi, A. Adachi, T. Matano, H. Akari, Improved capacity of a monkey-tropic HIV-1 derivative to replicate in cynomolgus monkeys with minimal modifications, Microbes Infect. 13 (2011) 58–64.
[30] M. Nomaguchi, M. Yokoyama, K. Kono, E.E. Nakayama, T. Shioda, A. Saito, H. Akari, Y. Yasutomi, T. Matano, H. Sato, A. Adachi, Gag-CA Q110D mutation elicits TRIM-independent enhancement of HIV-1mt replication in macaque cells, Microbes Infect. 15 (2013) 56–65.
[31] F. Bibollet-Ruche, A. Heigele, B.F. Keele, J.L. Easlick, J.M. Decker, J. Takehisa, G. Learn, P.M. Sharp, B.H. Hahn, F. Kirchhoff, Efficient SIVcpz replication in human lymphoid tissue requires viral matrix protein adaptation, J. Clin. Invest. 122 (2012) 1644–1652.
[32] M. Kawamura, T. Ishizaki, A. Ishimoto, T. Shioda, T. Kitamura, A. Adachi, Growth ability of human immunodeficiency virus type 1 auxiliary gene mutants in primary blood macrophage cultures, J. Gen. Virol. 75 (1994) 2427–2431.

Arch Virol (2013) 158:1209–1220
DOI 10.1007/s00705-013-1618-6

ORIGINAL ARTICLE

# Dynamics of cellular immune responses in the acute phase of dengue virus infection

**Tomoyuki Yoshida · Tsutomu Omatsu · Akatsuki Saito · Yuko Katakai · Yuki Iwasaki · Terue Kurosawa · Masataka Hamano · Atsunori Higashino · Shinichiro Nakamura · Tomohiko Takasaki · Yasuhiro Yasutomi · Ichiro Kurane · Hirofumi Akari**

Received: 13 June 2012 / Accepted: 12 December 2012 / Published online: 5 February 2013


**Abstract** In this study, we examined the dynamics of cellular immune responses in the acute phase of dengue virus (DENV) infection in a marmoset model. Here, we found that DENV infection in marmosets greatly induced responses of CD4/CD8 central memory T and NKT cells. Interestingly, the strength of the immune response was greater in animals infected with a dengue fever strain than in those infected with a dengue hemorrhagic fever strain of DENV. In contrast, when animals were re-challenged with the same DENV strain used for primary infection, the neutralizing antibody induced appeared to play a critical role in sterilizing inhibition against viral replication, resulting in strong but delayed responses of CD4/CD8 central memory T and NKT cells. The results in this study may help to better understand the dynamics of cellular and humoral immune responses in the control of DENV infection.

T. Yoshida and T. Omatsu contributed equally to this study.

**Electronic supplementary material** The online version of this article (doi:10.1007/s00705-013-1618-6) contains supplementary material, which is available to authorized users.

T. Yoshida · Y. Iwasaki · T. Kurosawa · M. Hamano · Y. Yasutomi · H. Akari
Tsukuba Primate Research Center, National Institute of Biomedical Innovation, 1-1 Hachimandai, Tsukuba, Ibaraki 305-0843, Japan

T. Yoshida (✉) · A. Saito · A. Higashino · H. Akari (✉)
Center for Human Evolution Modeling Research, Primate Research Institute, Kyoto University, Inuyama, Aichi 484-8506, Japan
e-mail: yoshida.tomoyuki.4w@kyoto-u.ac.jp

H. Akari
e-mail: akari.hirofumi.5z@kyoto-u.ac.jp

## Introduction

Dengue virus (DENV) causes the most prevalent arthropod-borne viral infections in the world [29]. Infection with one of the four serotypes of DENV can lead to dengue fever (DF) and sometimes to fatal dengue hemorrhagic fever (DHF) or dengue shock syndrome (DSS) [12]. The serious diseases are more likely to develop after secondary infection with a serotype of DENV that is different from that of the primary infection. Infection with DENV induces a high-titered neutralizing antibody response that can provide long-term immunity to the homologous DENV serotype, while the effect of the antibody on the heterologous serotypes is transient [22]. On the other hand, enhanced pathogenicity after secondary DENV infection appears to be explained by antibody-dependent enhancement (ADE). Mouse and monkey experiments have shown that subneutralizing levels of DENV-specific antibodies actually enhance infection [1, 6, 11]. Thus, the development of an effective tetravalent dengue vaccine is considered to be an important public-health priority. Recently, several DENV vaccine candidates have undergone clinical trials, and most of them target the induction of neutralizing antibodies [20].

T. Omatsu · T. Takasaki · I. Kurane
Department of Virology I, National Institute of Infectious Diseases, 1-23-1 Toyama, Shinjuku-ku, Tokyo 162-8640, Japan

Y. Katakai
Corporation for Production and Research of Laboratory Primates, 1-1 Hachimandai, Tsukuba, Ibaraki 305-0843, Japan

S. Nakamura
Research Center for Animal Life Science, Shiga University of Medical Science, Seta Tsukinowa-cho, Otsu, Shiga 520-2192, Japan

Research of the long-term immune response in humans has provided several interesting parallels to the data. It was reported that complete cross-protective immunity from heterologous challenge was induced in individuals 1–2 months after a primary DENV infection, with partial immunity present up to 9 months, resulting in a milder disease of shorter duration on reinfection, and that complete serotype-specific immunity against symptomatic dengue was observed up to 18 months postinfection [30]. Guzman and Sierra have previously recorded the long-term presence of both DENV-specific antibodies and T cells up to 20 years after natural infections [10, 31]. Of note, increased T cell activation is reportedly associated with severe dengue disease [7, 8]. Thus, the balance between humoral and cellular immunity may be important in the control of dengue diseases.

However, the details regarding the implication of humoral and cellular immunity in controlling DENV infection remain to be elucidated. Previously, passive transfer of either monoclonal or polyclonal antibodies was shown to protect against homologous DENV challenge [13, 15, 16]. It was also reported that neutralizing antibodies played a greater role than cytotoxic T lymphocyte (CTL) responses in heterologous protection against secondary DENV infection *in vivo* in IFN-α/βR$^{-/-}$ and IFNγR$^{-/-}$ mouse models [18]. Moreover, CD4$^{+}$ T cell depletion did not affect the DENV-specific IgG or IgM Ab titers or their neutralizing activity in the IFNγR$^{-/-}$ mouse model [36]. On the other hand, there are several reports showing that cellular immunity rather than humoral immunity plays an important role in the clearance of DENV. For example, in adoptive transfer experiments, although cross-reactive DENV-1-specific CD8$^{+}$ T cells did not mediate protection against a lethal DENV-2 infection, adoptive transfer of CD4$^{+}$ T cells alone mediated protection and delayed mortality in IFN-α/βR$^{-/-}$ and IFNγR$^{-/-}$ mouse models [39]. It has also been demonstrated that CD8$^{+}$ T lymphocytes have a direct role in protection against DENV challenge in the IFN-α/βR$^{-/-}$ mouse model of DENV infection by depleting CD8$^{+}$ T cells [35]. In addition, previous data from adoptive-transfer experiments in BALB/c mice showed that cross-reactive memory CD8$^{+}$ T cells were preferentially activated by the secondary DENV infection, resulting in augmented IFN-γ and tumor necrosis factor-α (TNF-α) responses, and this effect was serotype-dependent [2, 3]. Although it has previously been suggested that inducing neutralizing antibodies against DENV may play an important role in controlling DENV infection, CTLs are also proposed to contribute to clearance during primary DENV infection and to pathogenesis during secondary heterologous infection in the BALB/c mouse model [4].

Why did the mouse models of DENV infection show inconsistent results *in vivo*? One of the reasons could be that these results were obtained mainly from genetically manipulated mice such as IFN-α/βR$^{-/-}$ and IFNγR$^{-/-}$ mice. Moreover, these mice were inoculated with $10^{9}$–$10^{10}$ genome equivalents (GE) of DENV [27, 35, 36], which were likely in large excess compared with the $10^{4}$-$10^{5}$ GE of DENV injected into humans by a mosquito [19]. In addition, the efficiency of DENV replication in wild mice *in vivo* is very low compared to that in humans [35].

Recently, novel non-human primate models of DENV infection using rhesus macaques as well as marmosets and tamarins have been developed [24–26, 38]. An intravenous challenge of rhesus macaques with a high dose of virus inoculum ($1 \times 10^{7}$ GE) of DENV-2 resulted in readily visible hemorrhaging, which is one of the cardinal symptoms of human DHF [26]. It was also shown that the cellular immune response was activated due to expression of IFN-γ, TNF-α, and macrophage inflammatory protein-1 β in CD4$^{+}$ and CD8$^{+}$ T cells during primary DENV infection in rhesus macaques [20]. On the other hand, in the marmoset model of DENV infection, we observed high levels of viremia ($10^{5}$–$10^{7}$ GE/ml) after subcutaneous inoculation with $10^{4}$–$10^{5}$ plaque-forming units (PFU) of DENV-2. Moreover, we demonstrated that DENV-specific IgM and IgG were consistently detected and that the DENV-2 genome was not detected in any of these marmosets inoculated with the same DENV-2 strain used in the primary infection [24]. It is notable that while neutralizing antibody titers were at levels of 1:20-1:80 before the re-challenge inoculation, the titers increased up to 1:160-1:640 after the re-challenge inoculation [24]. These results suggested that the secondary infection with DENV-2 induced a protective humoral immunity to DENV-2 and that DENV-infected marmoset models may be useful in order to analyze the relationship between DENV replication and the dynamics of adaptive immune responses *in vivo*.

Taking these findings into consideration, we investigated the dynamics of cellular immunity in response to primary and secondary DENV infection in the marmoset model.

## Materials and methods

### Animals

All animal studies were conducted in accordance with protocols of experimental procedures that were approved by the Animal Welfare and Animal Care Committee of the National Institute of Infectious Diseases, Japan, and the National Institute of Biomedical Innovation, Japan. A total of six male marmosets, weighing 258–512 g, were used. Common marmosets were purchased from Clea Japan Inc.

(Tokyo, Japan) and caged singly at 27 ± 2 °C in 50 ± 10 % humidity with a 12-h light-dark cycle (lighting from 7:00 to 19:00) at Tsukuba Primate Research Center, National Institute of Biomedical Innovation, Tsukuba, Japan. Animals were fed twice a day with a standard marmoset diet (CMS-1M, CLEA Japan) supplemented with fruit, eggs and milk. Water was given ad libitum. The animals were in healthy condition and confirmed to be negative for anti-dengue-virus antibodies before inoculation with dengue virus [24].

## Cells

Cell culture was performed as described previously [24]. Vero cells were cultured in minimum essential medium (MEM, Sigma) with 10 % heat-inactivated fetal bovine serum (FBS, GIBCO) and 1 % non-essential amino acid (NEAA, Sigma) at 37 °C in 5 % $CO_2$. C6/36 cells were cultured in MEM with 10 % FBS and 1 % NEAA at 28 °C in 5 % $CO_2$.

## Virus

DENV type 2 (DENV-2) strain DHF0663 (accession no. AB189122) and strain D2/Hu/Maldives/77/2008NIID (Mal/77/08) were used for inoculation studies. The DENV-2, DHF0663 strain was isolated from a DHF case in Indonesia. The DENV-2 Mal/77/08 strain was isolated from imported DF cases from the Maldives. For all DENV strains, isolated clinical samples were propagated in C6/36 cells and were used within four passages on C6/36 cells. Culture supernatant from infected C6/36 cells was

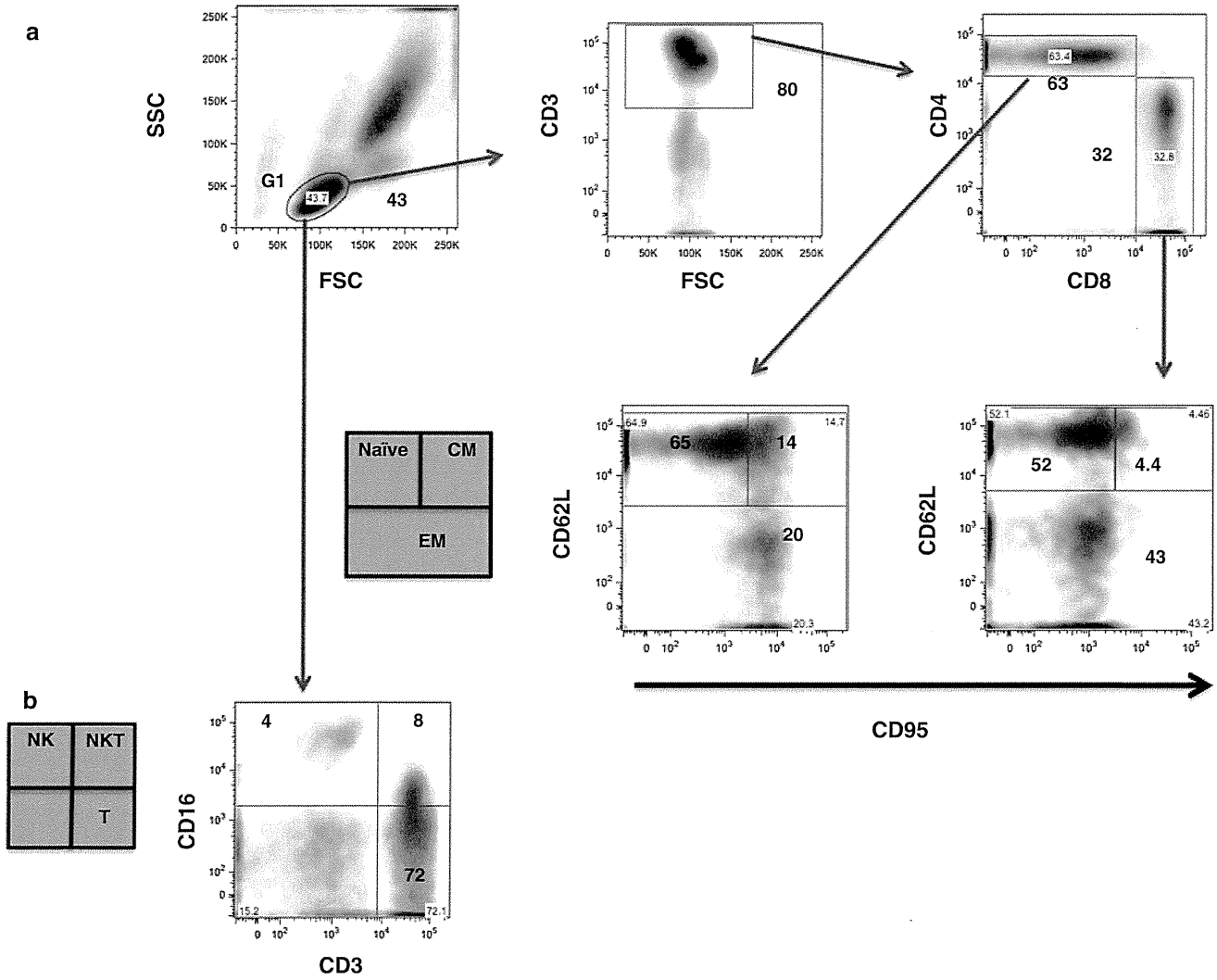


**Fig. 1 Flow cytometric analysis of naïve, central/effector memory T cells and NK/NKT cells in marmosets.** (**a**) Gating strategy to indentify CD4 and CD8 T, NK and NKT cells. The G1 population was selected and analyzed for CD4 and CD8 T, NK and NKT cells. (**a**) Profiling of naïve, central memory, and effector memory CD4 and CD8 T cells in total CD4 and CD8 T cells. (**b**) Profiling of NK and NKT cells in total lymphocytes. Results shown are representative of three healthy marmosets used in this study

centrifuged at 3,000 rpm for 5 min to remove cell debris and then stored at −80 °C until use.

### Infection of the marmosets with DENV

In the challenge experiments, profiling of the key adaptive and innate immune cells in the marmosets after infection with DENV-2 was done. For primary DENV infection, four marmosets were inoculated subcutaneously in the back with either $1.9 \times 10^5$ PFU of the DENV-2 Mal/77/08 strain (Cj08-007, Cj07-011) or $1.8 \times 10^4$ PFU of the DHF0663 strain (Cj07-006, Cj07-008) [24]. In the case of the DENV re-challenge experiment, two marmosets initially inoculated with $1.8 \times 10^5$ PFU of the DHF0663 strain were re-inoculated 33 weeks after the primary challenge with $1.8 \times 10^5$ PFU of the same strain (Cj07-007, Cj07-014) [24]. Blood samples were collected on days 0, 1, 3, 7, 14, and 21 after inoculation and were used for virus titration and flow cytometric analysis. Inoculation with DENV and blood drawing were performed under anesthesia with 5 mg/kg of ketamine hydrochloride. Day 0 was defined as the day of virus inoculation. The viral loads in marmosets obtained in a previous study are shown in Supplementary Figure 1 [24].

### Flow cytometry

Flow cytometry was performed as described previously [37]. Fifty microliters of whole blood from marmosets was stained with combinations of fluorescence-conjugated monoclonal antibodies; anti-CD3 (SP34-2; Becton Dickinson), anti-CD4 (L200; BD Pharmingen), anti-CD8 (CLB-T8/4H8; Sanquin), anti-CD16 (3G8; BD Pharmingen), anti-CD95 (DX2; BD Pharmingen), and anti-CD62L (145/15; Miltenyi Biotec). Then, erythrocytes were lysed with FACS lysing solution (Becton Dickinson). After washing with a sample buffer containing phosphate-buffered saline (PBS) and 1 % FBS, the labeled cells were resuspended in a fix buffer containing PBS and 1 % formaldehyde. The expression of these markers on the lymphocytes was analyzed using a FACSCanto II flow cytometer (Becton Dickinson). The data analysis was conducted using FlowJo software (Treestar, Inc.). Results are shown as mean ± standard deviation (SD) for the marmosets used in this study.

**Table 1** Subpopulation ratios of lymphocytes in marmosets

| Subpopulation name | Subpopulation ratios (Mean ± SD: %) |
|---|---|
| $CD3^+$ | 75.7 ± 6.4 |
| $CD3^+CD4^+$ | 65.4 ± 6.8 |
| $CD3^+CD4^+CD62L^+CD95^-$ (CD4 $T_N$) | 65.9 ± 3.7 |
| $CD3^+CD4^+CD62L^+CD95^+$(CD4 $T_{CM}$) | 16.4 ± 2.9 |
| $CD3^+CD4^+CD62LCD95^\pm$ (CD4 $T_{EM}$) | 19.5 ± 2.5 |
| $CD3^+CD8^+$ | 29.0 ± 8.0 |
| $CD3^+CD8^+CD62L^+CD95^-$ (CD8 $T_N$) | 66.7 ± 10.2 |
| $CD3^+CD8^+CD62L^+CD95^+$(CD8 $T_{CM}$) | 4.7 ± 3.6 |
| $CD3^+CD8^+CD62LCD95^\pm$ (CD8 $T_{EM}$) | 28.8 ± 14.8 |
| CD3CD16 + (NK) | 4.2 ± 2.6 |
| $CD3^+CD16^+$ (NKT) | 5.1 ± 3.4 |

SD: Standard deviation

Results shown are mean ± SD from 3 healthy marmosets

## Results

### Naïve central/effector memory T cells and NK/NKT cells in marmosets

Basic information regarding CD4/CD8 naïve and central/effector memory T cells and NK/NKT cells in common marmosets was unavailable. Thus, we examined the immunophenotypes of lymphocyte subsets in the marmosets (Fig. 1). The gating strategy for profiling the CD4 and CD8 T cells in the marmosets by FACS is shown in Fig. 1a. Human T cells are classically divided into three functional subsets based on their cell-surface expression of CD62L and CD95, i.e., $CD62L^+CD95^-$ naive T cells ($T_N$), $CD62L^+CD95^+$ central memory T cells ($T_{CM}$), and $CD62L^-CD95^\pm$ effector memory T cells ($T_{EM}$) [9, 21, 28]. In this study, $CD4^+$ and $CD8^+$ $T_N$, $T_{CM}$, and $T_{EM}$ subpopulations were defined as $CD62L^+CD95^-$, $CD62L^+CD95^+$, and $CD62L^-CD95^\pm$, respectively (Fig. 1a and Table 1). The average ratio of $CD3^+$ T lymphocytes in the total lymphocytes of three marmosets was found to be 75.7 ± 6.4 %. The average ratio of $CD4^+$ T cells in the $CD3^+$ subset was 65.4 ± 6.8 %. The average ratios of $CD4^+$ $T_N$, $T_{CM}$, and $T_{EM}$ cells were 65.9 ± 3.7 %, 16.4 ± 2.9 %, 19.5 ± 2.5 %, respectively. The average ratio of $CD8^+$ T cells in the $CD3^+$ subset was 29.0 ± 8.0 %. The average ratios of $CD8^+$ $T_N$, $T_{CM}$, and $T_{EM}$ cells were 66.7 ± 10.2 %, 4.7 ± 3.6 %, 28.8 ± 14.8 %, respectively.

We recently characterized a $CD16^+$ major NK cell subset in tamarins and compared NK activity in tamarins with or without DENV infection [37, 38]. In terms of NKT cells, NK1.1 (CD161) and CD1d are generally used as markers of NKT cells [32]. However, these anti-human NK1.1 and CD1d antibodies are unlikely to cross-react with the NKT cells of the marmosets. Thus, we defined NKT cells as a population expressing both CD3 and CD16 as reported previously [14, 17]. The NK and NKT cell subsets were determined to be $CD3^-CD16^+$ and $CD3^+CD16^+$ lymphocytes in the marmosets. The average ratios of NK and NKT cell subsets in the lymphocytes were 4.2 ± 2.6 % and 5.1 ± 3.4 %, respectively (Table 1). We observed that the proportions of the major lymphocyte

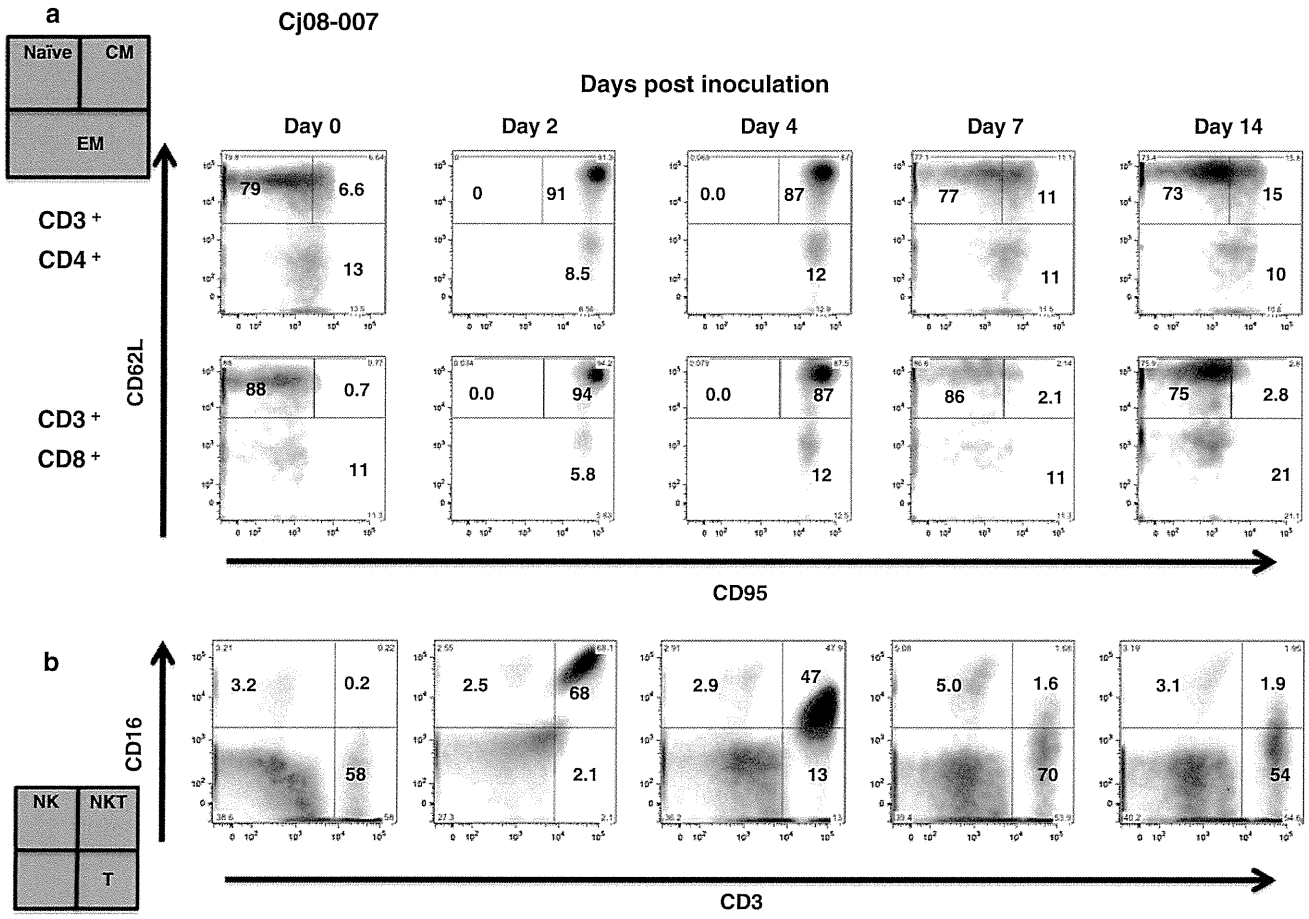


**Fig. 2 Profiling of CD4 and CD8 T, NK and NKT cells in marmosets with primary infection with the DENV-2 Mal/77/08 strain.** For primary DENV infection, two marmosets were inoculated subcutaneously in the back with $1.9 \times 10^5$ PFU of the DENV-2 Mal/77/08 strain. (**a**) Profiling of naïve, central memory, and effector memory CD4 and CD8 T cells in total CD4 and CD8 T cells. (**b**) Profiling of NK and NKT cells in total lymphocytes. (**a-b**) Cj08-007

subsets in the marmosets were similar to those in cynomolgus monkeys and tamarins [37, 38].

## Profiling of CD4 and CD8 T, NK and NKT cells in marmosets after primary infection with DENV-2 (Mal/77/08 strain)

We investigated the cellular immune responses against DENV-2 DF strain (Mal/77/08) in marmosets. Dengue vRNA was detected in plasma samples from two marmosets on day 2 postinfection (Supplementary Fig. 1a). For the two marmosets (Cj08-007, Cj07-011), the plasma levels of vRNA reached their peaks at $9.6 \times 10^6$ and $7.0 \times 10^6$ GE/ml, respectively, on day 4 postinfection. Plasma vRNA was detected in both marmosets on days 2, 4, and 7. We then examined the profiles and frequencies of the CD4 and CD8 T, NK and NKT cells in the infected marmosets (Figs. 2–3 and Table 2). $CD4^+$ $T_{CM}$ cells drastically increased to 88.7 ± 2.8 % from 13 ± 0.4 % between day 0 and day 2 post-inoculation (Table 2). Reciprocally, $CD4^+$ $T_N$ cells decreased to 1.6 ± 3.3 % from 74.1 ± 0.9 % at the same time. $CD4^+$ $T_{EM}$ cells maintained the initial levels throughout the observation period. $CD8^+$ $T_{CM}$ cells increased to 91.9 ± 5.5 % from 2.1 ± 0.8 % between day 0 day 2 post-inoculation, and reciprocally, $CD8^+$ $T_N$ cells decreased to 2.5 ± 4.7 % from 89.9 ± 2.5 % at the same time. In addition, NK cells maintained their initial levels throughout the observation period. However, NKT cells drastically increased to 52.6 ± 17 % from 0.2 ± 0.0 % between day 0 and day 2 post-inoculation. These results suggest that CD4/CD8 T and NKT cells may efficiently respond to the Mal/77/08 strain of DENV.

## Profiling of CD4 and CD8 T, NK and NKT cells in the marmosets after primary infection with DENV-2 (DHF0663 strain)

Next, we investigated cellular immune responses against another DENV-2 DHF strain (DHF0663) in marmosets.